

LATERAL LOAD TESTING OF MODEL PILES - PHASE 1

by

Joseph A. Caliendo

Loren R. Anderson

Utah State University

Department of Civil and Environmental Engineering

March 1996

Acknowledgments

The authors wish to express their gratitude to the Utah Department of Transportation and to the Mountain-Plains Consortium for providing the financial assistance which made this project possible. The authors also acknowledge the significant contributions made to this research by Utah State University graduate students Steve Dapp, Mark Rawlings and Robb Moss. Mr. Rene Winward provided invaluable technical assistance, including design and fabrication of the strain gauge installation tool.

Disclaimer

The contents of this report reflect the views of the authors, who are responsible for the facts and the accuracy of the information presented herein. This document is disseminated under the sponsorship of the Department of Transportation, University Transportation Centers Program, in the interest of information exchange. The U.S. Government assumes no liability for the contents or use thereof.

ABSTRACT

Utah State University is currently involved with a research project funded by the Utah Department of Transportation and the Mountain-Plains Consortium. The reaction of model piles subjected to lateral loading is the subject of ongoing research. The measured response of laterally loaded model pile is compared with predicted results. The model piles are 60 inches long. Approximately 48 inches of which is embedded in a soft clay soil. The piles consist of one inch schedule 40, (1.315 in. OD) aluminum tubes, with a wall thickness of 0.331 inch.

In order to measure the pile response to the lateral loads, the test pile was instrumented with 14 pairs of foil strain gages mounted at 3.75 inch spacings. The gage pairs were mounted on the inside wall of the seamless tube. A special installation tool was designed and fabricated at Utah State for this purpose. A wedge/scissors device was used to mount the strain gages to the inside wall.

The strain gages (CEA - 13-250UW-120) are each wired into a 1/4 Wheatstone bridge circuit with a “dummy” temperature gage. The 28 two-wire leads, along with LVDT leads, are routed through a multiplexer to a 21x data logger.

The pile calibration and load test results are discussed. The measured moments compared very favorably to those predicted by LPGSTAN and COM624P.

TABLE OF CONTENTS

BACKGROUND	1
WORK PLAN	2
Phase 1 (present)	2
Phase 2 (future)	2
Phase 3 (future)	2
OBJECTIVES (Phase 1)	3
TEST FACILITY	3
MODELING CONSIDERATIONS	4
Prototype Pile	4
Similitude	5
Model Pile	6
INSTRUMENTATION	8
Strain Gage Installation	8
Instrumentation Circuitry	9
Data Acquisition System	9
CALIBRATION RESULTS	10
Load Test Program	11
LOAD TEST RESULTS	13
Moment	13
Pile Top Deflection	14
p-y Curves	14
Measured versus Predicted Behavior	15
Pile Moment	16
Pile Top Movement	16
CONCLUSIONS	16
REFERENCES	17
APPENDIX: Calibration Curves for Each Strain Gage	57

LIST OF TABLES

Table 1.	Similitude Considerations	5
Table 2.	Prototype and Model Characteristics	7
Table 3.	Calibration Loads and Associated Stresses	11
Table 4.	Load Test Program	12

LIST OF FIGURES

Figure 1.	Utah State University Model Test Facility	19
Figure 2.	Simplified Hydraulic Schematic	20
Figure 3.	Model Pile and Strain Gage Locations	21
Figure 4.	Utah State University Strain Gage Installation Tool	22
Figure 5.	Photographs Showing Strain Gage Installation	23
Figure 6.	Wheatstone Bridge	24
Figure 7.	Data Acquisition System	25
Figure 8.	Calibration Loadings	26
Figure 9.	Calibration Curve, Strain Gage #7, Black	27
Figure 10.	Calibration Curve, Strain Gage #7, Red	28
Figure 11.	Moment vs. Depth, Test #1, Beginning of Time Interval	29
Figure 12.	Moment vs. Depth, Test #1, Middle of Time Interval	30
Figure 13.	Moment vs. Depth, Test #1, End of Time Interval	31
Figure 14.	Moment vs. Depth, Test #2, Beginning of Time Interval	32
Figure 15.	Moment vs. Depth, Test #2, Middle of Time Interval	33
Figure 16.	Moment vs. Depth, Test #2, End of Time Interval	34
Figure 17.	Moment vs. Depth, Test #3, Beginning of Time Interval	35
Figure 18.	Moment vs. Depth, Test #3, Middle of Time Interval	36
Figure 19.	Moment vs. Depth, Test #3, End of Time Interval	37
Figure 20.	Moment vs. Depth, Test #1, Eng of Time Interval — Minimum, Mid Range, and Maximum Lateral Load	38
Figure 21.	Measured Pile Top Displacement vs. Applied Lateral Loads, Tests 4, 5, & 6	39
Figure 22.	Measured Pile Top Slope vs. Applied Lateral Loads, Tests 4, 5, & 6	40
Figure 23.	Best Fit Polynomial for Moment Distribution, Lateral Load, 41.6 lbs	41
Figure 24.	Best Fit Polynomial for Moment Distribution, Lateral Load, 74.3 lbs	42
Figure 25.	Best Fit Polynomial for Moment Distribution, Lateral Load, 114.2 lbs	43
Figure 26.	Best Fit Polynomial for Moment Distribution, Lateral Load, 146.9lbs	44
Figure 27.	Best Fit Polynomial for Moment Distribution, Lateral Load, 179.5 lbs	45
Figure 28.	Best Fit Polynomial for Moment Distribution, Lateral Load, 223.1 lbs	46

Figure 29.	Best Fit Polynomial for Moment Distribution, Lateral Load, 255.8 lbs	47
Figure 30.	Best Fit Polynomial for Moment Distribution, Lateral Load, 266.7 lbs	48
Figure 31.	P-y Curve at Depth of 29.75 inches	49
Figure 32.	Undrained Shear Strength of Model Clay Soil, Tests 1, 2, & 3	50
Figure 33.	Undrained Shear Strength of Model Clay Soil, Tests 4, 5, & 6	51
Figure 34.	Measured Moments vs. Predicted Moments Lateral Load, 41.6 lbs	52
Figure 35.	Measured Moments vs. Predicted Moments Lateral Load, 146.9 lbs.	53
Figure 36.	Measured Moments vs. Predicted Moments Lateral Load, 179.5 lbs	54
Figure 37.	Measured Moments vs. Predicted Moments Lateral Load, 266.7 lbs	55
Figure 38.	Measured and Predicted Pile Top Displacement vs. Lateral Loads	56

EXECUTIVE SUMMARY

Lateral loading on piles and drilled shafts often controls the design of these foundation systems. LPGSTAN is a 3-D, non-linear, finite element analysis program written at the University of Florida and endorsed by the Federal Highway Administration for use in designing piles and pile groups subjected to lateral loads. Validation of this software with lateral load tests is essential, but due to high expense, full-scale load test data is limited.

This project is an effort to validate the LPGSTAN program using model piles in lateral load tests. The objectives of Phase 1 of this project were to:

1. Develop a load test facility which can be used to perform static lateral load tests on model piles.
2. Establish a prototype pile and a corresponding model pile.
3. Design and implement the instrumentation for the model pile.
4. Calibrate the model pile.
5. Perform lateral load tests on the model pile.
6. Reduce the load test data and establish stresses, moments, and deflections from the measurements.
7. Compare measured response to predictions made with LPGSTAN.

The load test facility consists of a 10 ft. by 3 ft. by 4.5 ft. deep tank that was filled with a saturated silty clay soil. The soil was consolidated in the tank by means of ten hydraulic cylinders; constant pressure was maintained with a hydraulic accumulator.

UDOT commonly uses steel pipe piles that are 12.75 in. OD with a 3/8 inch wall thickness. A pipe pile with these dimensions was chosen as the prototype pile. The model pile was sized using the prototype pile dimensions and similitude, which resulted in selecting a Schedule 40, 6061-T6 aluminum

pipe with an OD of 1.315 inch and a wall thickness of 0.133 inch for the testing. This size effectively utilizes the 54 inches of test soil by requiring an embedment length of 44.6 inches. In order to measure the response of the model piles to lateral loads, 14 pairs of strain gages were mounted diametrically opposed on the interior surface of the aluminum pipes at a spacing of 3.75 inches. Strain gage measurements were taken by a Campbell Scientific 21X Data logger after multiplexing the excitation voltage through a Wheatstone bridge. The data was then sent to a computer. An LVDT attached to pile top recorded the pile displacement during the tests.

Before actual testing, each of the piles was calibrated by loading them as a simply supported beam. Two loading configurations were used: a concentrated load at the center and two symmetric concentrated loads spaced between the supports and the center point of the pile. The measured stresses were plotted against the calculated stresses, and a calibration factor was determined for each gage of each pile.

Three lateral load tests, designated as Test 1, Test 2 and Test 3 were performed on July 23-24, 1995, according to ASTM standard D 3966-81. After the pile had been pushed into the test soil, the loads were applied horizontally at 6 inches above the soil surface by a cable and pulley system. The loads ranged from 41.61bf. To 266.71bf. based on percentages of a prototype design load. Strain gage readings were taken at the beginning, middle, and end of each load/time increment. For Test 2, the pile was loaded in the opposite direction as Test 1, and the loading was again reversed for Test 3.

The raw data recorded by the data logger was imported into a spreadsheet and strains and corresponding stresses were calculated for each measured location in the model pile. A moment distribution was then plotted over the length of the pile. From the moment distribution curves, the point of fixity of the pile can be seen to move down as the load increases, and the maximum load causes "short

pile" behavior. For further testing, Tests 4, 5, and 6 used identical loading procedures, but two LVDT's were used to measure pile top displacement.

Using the properties of the test facility soil in the computer programs LPGSTAN and COM624P, the predicted pile behavior was compared with the model results. The measured moments from Tests 1, 2, and 3 closely matched the predicted results from both LPGSTAN and COM624P, and the pile top displacement results from the tests compare fairly well with the computer predictions.

When comparing the accomplishments of this project with the Phase 1 objectives, one can conclude that this phase of the project has been very successful. A test facility, model pile and reliable testing instrumentation and data collection system has been developed. The LPGSTAN computer model was verified for a single pile subjected to lateral loading. The experience gained from Phase 1 will be invaluable for the continuing research involving pile groups and cyclic loading.

BACKGROUND

Highway bridges are very often supported on deep foundations (ie. driven piles and/or drilled shafts). These foundations must be designed to resist both axial forces and lateral forces. The lateral forces often control the design of these foundation systems. There are several sophisticated computer models available for predicting the response of piles and pile groups subjected to lateral loading. One such program being funded and endorsed by the Federal Highway Administration for State Highway Department's use is LPGSTAN, a 3-D, non-linear, finite element analysis program written at the University of Florida, McVay (1993). This is a result of increased concern over pile foundations being subjected to extreme lateral events such as earthquakes, ship impact, and scour. LPGSTAN can model pile groups (including battered piles) and is capable of modeling a wide variety of loads and moments applied to the pile cap and/or super-structure.

It is essential that these predicted computer results be validated by comparison with measured results. Because of the very high expense, limited full scale lateral load test data is available particularly for pile groups. To date, only two such tests are well documented. These occurred at the University of Houston and coastal California. The Federal Highway Administration was involved with funding for both of these past projects. Lateral response of pile groups remains a very high priority, not only for the Utah Department of Transportation, but also with the Federal Highway Administration and the Transportation Research Board (TRB).

The state of Utah is experiencing significant growth and a corresponding increase in its infrastructure particularly along the Wasatch Front's I-15 corridor. If this design package can be validated for characteristic Utah soils, it can be used with greater confidence by UDOT in the design of deep foundations.

WORK PLAN

The UDOT Technical Advisory Committee (TAC) and USU decided that the best way for approaching the problem was to break the overall project into distinct phases. The phases are:

Phase 1 (present)

Develop & implement a load test facility for performing model lateral load tests on a single pile. This report completes phase 1 of the project. The ongoing phase 1 progress has been documented previously via:

- Northwest Geotechnical Workshop, FHWA/UDOT Big Fork Montana August 1994
- US Taiwan Geotechnical Engineering Collaboration Workshop, Taiwan R.O.C.
January 1995
- Interim report to UDOT, February 1995
- Engineering Geology and Geotechnical Engineering Symposium, USU March 1995
- Load test demonstration for UDOT, September 1995
- Presentation to TRB Committee A2K03, Washington DC, January 1995
- Paper accepted for presentation at 1996 TRB Meeting
- Presentation to TRB Committee A2K03, Washington DC, January 1996
- Presentation at AASHTO Bridge meeting, Portland Oregon

Phase 2 (future)

Develop equipment and testing procedures for model pile groups and cyclic loading.

Phase 3 (future)

Verify model pile group response through full scale load testing of pile groups.

OBJECTIVES (Phase 1)

The objectives of phase 1 were to:

- 1) Develop a load test facility, which can be used to perform static lateral load tests on model piles.
- 2) Establish a prototype pile and a corresponding model pile.
- 3) Design and implement the instrumentation for the model pile.
- 4) Calibrate the model piles.
- 5) Perform lateral load tests on the model pile.
- 6) Reduce the load test data and establish stresses, deflections, moments, and p-y data from the measurements.
- 7) Compare measured response to predictions made with computer program LPGSTAN.

TEST FACILITY

The test facility consists of a ribbed steel tank 10 ft by 3 ft in plan, and 4 ft deep as shown in Figure 1. An impermeable liner retains the water to keep the soil saturated, while the geocomposite between the liner and the soil provides a drainage path to expedite the consolidation process.

The test soil was consolidated in the tank by means of ten hydraulic rams, on five yokes, with each ram having a diameter of 4 inches. An effective overburden stress is simulated with hydraulic pressure according to the relationship:

$$\sigma' = \frac{(10 \text{ cylinders}) * P * (3.14159) * (2 \text{ inches})^2}{(10 \text{ ft} * 3 \text{ ft})}$$

where:

σ' = effective consolidating stress

P = hydraulic pressure (psi)

H = height of simulated, saturated overburden (feet)

g = unit weight's (pcf)

(10 ft) *(3 ft) = soil area in plan view

The hydraulic system initially consisted of a pump supplying pressure to the cylinders through a four-way slide valve with the return (drainage) being dumped to a sump. The valve could be opened, and the cylinders pressurized to a desired level providing a load to the soil. However, once the valve was closed the pressure dropped off very rapidly as a result of the load plate moving away from the ram feet into the yielding soil surface. Thus the hydraulic consolidation pressure consisted of nearly instantaneous spikes that dropped off very rapidly.

It was necessary to incorporate a hydraulic accumulator into the system in order to maintain a constant consolidating pressure to the clay soil, and for the load plate to "follow" the soil downward as it consolidated. This was accomplished, and the new hydraulic system was operational on November 14, 1994, and has performed satisfactorily. Any desired constant hydraulic consolidation pressure may be maintained within about ± 5 psi. The load plate now follows the soil down as consolidation progresses. Figure 2 contains simplified hydraulic schematics, both before and after the accumulator was added.

MODELING CONSIDERATIONS

In order to have the model pile represent a realistic prototype, the model pile was dimensionally scaled in accordance with similitude considerations.

Prototype Pile

The prototype pile is a 323.85 mm OD (12.75 in.) steel pipe with 7.94 mm wall thickness (0.3125 in.) and an end cap. This is a pile that is commonly used for UDOT projects. It is not essential that a strict parallelism be maintained between model and prototype because the results of the model pile tests will be compared to predictions made by the design package LPGSTAN. Once this design package is validated for characteristic Utah clay soils and piles it can be used with greater confidence for designs in this area.

The pile length was determined by performing lateral load analyses of the prototype pile. For long piles, the maximum moment and pile top deflection are independent of the pile length and remain constant. Successive analyses were performed with decreasing pile lengths until moment and deflection were affected by pile length. The prototype pile length was established in this fashion as approximately 10.98 m (36 ft).

Similitude

There are seven fundamental variables (F.V.) of interest. These fundamental variables contain only the two basic dimensions (B.D.) of force (F) and length (L), as summarized in Table 1.

Table 1. Similitude Considerations

Fundamental Variable	Basic Dimensions
Δ Pile Deflection	L
P Applied Lateral Load	F
D Outside Pile Diameter	L
L Pile Length	L
EI Pile Stiffness	FL^2
C Soil Cohesion	F/L^2
H Height of Applied Load	L

There are five required Pi terms (F.V. minus B.D.). Since deflection (Δ) is the variable of

$$\frac{\Delta}{D} = f \left[\frac{PD^2}{EI}, \frac{L}{D}, \frac{L}{H}, \frac{CD^4}{EI} \right]$$

interest, it is the non-repeating variable, and is a function of the other four Pi terms as shown below.

The scale factors are established by equating the model Pi terms with the prototype Pi

terms (ie. $(L/D)_m = (L/D)_p$..etc). It is important to realize that since the undrained shear strength is not a function of soil stress, the test soil can be established as the prototype soil (i.e. the undrained shear strength need not be scaled). The diameter (D) is fixed once the length (L) of the model pile is established by the Pi term L/D (also, H is fixed by H/L). However, the wall thickness, and subsequently the cross-sectional moment of inertia (I), is still independent at this point. This allows for the use of wall thickness to control model pile stiffness (EI) to yield a manageable model lateral load.

The smaller the model pile stiffness, the smaller (and more manageable) the model lateral load needed to simulate a full-scale load according to the Pi term PD^2/EI . The length of the model pile must be limited such that it extends no closer than three pile diameters of the bottom of the test bin to minimize boundary effects.

The second way of controlling model pile stiffness (EI), and thus, the model lateral load needed (P), is through the model pile material (E). By using a model pile with a material with a lower modulus of elasticity (E), a smaller model load can simulate the given full scale load. The danger of getting too low of a modulus of elasticity (E) is that its yield stress and stability against crimping failure are also reduced. The strain gages can be mounted on any metallic surface.

Model Pile

After having established a prototype pile and subsequent similitude analyses, the physical characteristics of the model pile were determined. It is necessary to choose dimensions and characteristics for the model pile that are both consistent with the similitude analyses and still readily available. These are shown in Table 2. Given the dimensions shown in this table, the following scaling relationships are established:

$$P_p = 98.6 * P_m \quad \Delta_p = 9.7 * \Delta_m$$

Where P is the applied lateral load on the model and prototype and Δ is the deflection of model and prototype.

Table 2. Prototype and Model Characteristics

Property	Prototype	Model
Material	Steel Pile	Aluminum Tube
D	323.85 mm (12.75 in.)	33.40 mm (1.315 in.)
E	200 gPa (29,000 ksi)	70 gPa (10,000 ksi)
L	10.98 m (36 ft)	1132.84 mm (44.6 in.)
I	11625.3 cm ⁴ (279.3 in. ⁴)	3.63 cm ⁴ (0.08734 in. ⁴)
P	89.0 kN (20,000 lbf)	0.903 kN (203 lbf)
C	Same	Same

The model pile material is 6061 T6 aluminum conforming to ATSM B 241. A schedule 40 tube (1.315 inch OD, and 0.133 inch wall thickness) was chosen from the available standard sizes. This size effectively utilizes the 1.22m (4.0 ft) depth of test soil available by requiring a length of embedment of 1.13m (44.6 in.). A lateral load of 0.903 kN (203 lbf) on the model corresponds to a lateral load of 89.0kN (20,000 lbf) on the prototype pile.

A preliminary analysis showed that the point of fixity (critical length for a long, counterflexured pile) is less than 1.016m (40 in.). The maximum anticipated stress is only about one third of the aluminum's yield stress. The ratio of OD to thickness is relatively small and a crimping failure is not anticipated.

INSTRUMENTATION

In order to measure the response of the model pile to the applied lateral loads, some unique instrumentation was developed. Strain gages were installed on the inside surface of the model pile and a linear variable deformation transformer (LVDT) was used to measure the pile top deflection.

Strain Gage Installation

Fourteen pairs of bonded resistance type strain gages (CEA - 13- 250UW-120) were mounted along the inside surface of the aluminum model pile without splitting the pile. The strain gage pairs were installed at the intervals shown in Figure 3 by means of the specialty tool shown in Figure 4, designed and machined at the USU Civil Engineering machine shop. The tool is inserted into the pile by means of two telescoping rods (not shown). The outer rod holds the tool at the exact required location and the inner rod engages the screw and wedge assembly. The wedge forces the wings apart. The wings press the two strain gages against diametrically opposite sides on the inside wall of the tube and hold the gages in place while the epoxy cures. This takes approximately 6 hours. The purpose of the rubberband is to assist in collapsing the wings as the wedge is withdrawn. The sequence of installation steps was as follows:

- Degreased inside of tube
- Polished inside with steel wool and acid conditioner
- Flushed with neutralizer and dry air
- Inserted installation tool and applied strain gages with M bond AE-10 adhesive

The 28 gages were mounted, two at a time, by inserting the tool through the pile bottom and installing the gages beginning at the pile top. This is shown in the photograph in Figure 5. The lead wires were soldered to the strain gages prior to installation. The 56 lead wires were pulled through the pile top

and bundled together. After all the gages were installed, the tubes were purged with nitrogen gas and the ends were sealed off. This was done in order to safeguard against moisture collecting inside the tubes.

Instrumentation Circuitry

Strains are measured by placing the active strain gage in a four-arm Wheatstone bridge circuit as shown in Figure 6. To compensate for temperature induced strains, a “dummy” gage is also connected into the Wheatstone bridge circuit. The dummy gage was mounted on a separate unstressed model pile which was subjected to the same environmental conditions as the active gage. This canceled the environmental (temperature induced) strains leaving only the strains caused by the external loading. The same Wheatstone bridge arrangement was repeated for each of the 28 gages and separate readings were taken on each. Measuring the total strain at diametrically opposite positions on the model pile also provides both axial and bending strains.

Data Acquisition System

The data acquisition system consisted of a Campbell Scientific Inc. 21X datalogger, an AM 416 relay multiplexer, and an IBM compatible 386 computer. For a given applied lateral load, the response of the pile at each of the 28 strain gage locations was measured and stored. In addition to the strain gage measurements, an LVDT measurement was also recorded at the pile top. A schematic of the data acquisition system is shown in Figure 7.

Automated conversion of the electronic sensor signals to a digital value was performed by the 21 X datalogger. The programmable datalogger supplied a predetermined excitation (supply) voltage to a sensor (i.e. strain gage or LVDT) through internal bridge configurations. The supply and output voltages, V_s and V_o were precisely measured and processed by the datalogger. The strain gage factor, S , is a constant. The relationship between voltage and strain

$$\epsilon = \frac{V_0(R_2 + R_{3i})^2}{V_s S R_2 R_{3i}}$$

for the circuitry involved is as follows:

Since the number of sensors exceeds the number of available datalogger input channels, it was necessary to multiplex the analog sensor signals using the AM 416 relay multiplexer. The multiplexer was positioned between the sensors and the datalogger. Mechanical relays are used to switch the sensor signals through the system. The operation of the multiplexer was controlled by the datalogger in the datalogger program.

CALIBRATION RESULTS

Before performing an actual load test on the model pile, it was necessary to calibrate each of the strain gages. Since this study was to measure the response of the model piles to lateral loads, the calibration was done by loading the pile as a simple beam as shown in Figure 8. The measured stresses were then compared with the calculated response of the pile. There are various reasons why the measured stresses are not likely to exactly match the calculated stresses. These include, but are not limited to, the following:

- Gage pairs not being mounted exactly diametrically opposite each other
- Strain gages not being in perfect longitudinal and/or radial alignment
- Variations in wall thickness of the model pile

- Unaccounted electrical voltage potentials in the circuitry
- Modulus of Elasticity different than assumed value

Various load configurations were used for calibration. The pile was loaded in bending with a concentrated load at the middle, with symmetric concentrated loads, and axially in compression. Each gage was subjected to tensile and compressive bending stresses as well as axial compression stress. The calibration loads were chosen to ensure that the resulting stresses exceeded the anticipated stresses but remained less than the yield stress of the aluminum tube. Several measurements were made at each gage for each load. The stress was monitored using the data acquisition system and the results were downloaded to a spreadsheet. The measured stress was plotted against the calculated stress. These plots were made for each gage and are the basis for the calibration factors.

Since the strain and stress were directly proportional at the imposed stress levels, the measured stress σ_M was plotted against the calculated stress, σ_C . The data points formed a very narrow envelope. A regression analysis was done using the measured stress as the dependent variable. A calibration factor (regression coefficient) was then determined which modified the measured stresses to match the calculated stresses. A calibration curve of σ_M versus σ_C was developed for each strain gage. Figures 9 and 10 show the calibration relationship developed for 13 the gage pair at location 7. The calibration curves for each gage are shown in the appendix. The ranges of stress imposed on the pile by the different calibration loads are shown in Table 3. The axial compressive stresses plot over a relatively narrow range. The maximum stresses were approximately 80 percent of the model pile's yield stress.

Table 3. Calibration Loads and Associated Stresses

Maximum Calibration Load	Maximum Stress
Symmetric Concentrated Loads 1821bs (each load)	Bending 17400 psi
Concentrated Load @ Center 175 lbs	Bending 15600 psi

Axial Load 1521bs	Axial Compression 310 psi
-------------------	---------------------------

Load Test Program

Three lateral load tests were performed on July 23-24, 1995, in general accordance with ASTM D 3966-81. This standard designates the applied lateral load in terms of a design load (DL). Table 4 shows the lateral load and time duration for each load increment. These load tests consisted of applying a horizontal load to the pile at a point 6 inches above the soil surface. After the first test was completed, the pile was loaded in the reverse direction and tested. The loading direction was again reversed for the third test. The tests are designated Test 1, 2, and 3. Each test was completed in approximately seven hours. This included testing and setup time.

Three additional tests were performed on September 19-20, 1995, designated as Tests 4, 5, and 6. The data from these tests have not yet been completely reduced. The model pile was recalibrated prior to testing to ensure that the calibration results were repeatable, which they were. Testing was done in exactly the same manner as the first set of tests with the exception that a second LVDT was added to measure the slope at the pile top. The additional LVDT was used to define both deflection and slope at the top of the pile for use as a boundary condition for computing p-y curves.

Table 4. Load Test Program

Lateral Load (lbs)	Duration (minutes)	Lateral Loads (lbs)	Duration (minutes)
41.6	10	255.8	20
74.3	10	266.7	60
114.2	10	190.4	10
146.9	15	125.1	10
179.5	20	63.4	10
223.1	20	0	

Three measurements were made at the beginning, middle, and end of each load step. Since there are 28 strain gages and one LVDT gage, this was 261 measurements made for each load increment. The Campbell Scientific Data Logger and Multiplexer provided for efficient data acquisition. The raw data was imported into a spreadsheet for subsequent calculations. Three readings were taken at each time step and an average taken in order to mitigate the electrical circuitry “noise.” The most significant readings are those taken at the end of the time interval since, by then, the pile movement had stopped. The raw data actually consists of the ratio of output voltage to input voltage at each strain gage. An initial voltage ratio is established 15 under no load conditions. This is subtracted from subsequent readings and the corresponding strain is calculated using the previous equation..

When possible, the strains and corresponding stresses were calculated from the average values of the strain gage pairs. The single Wheatstone bridge circuitry provides for redundancy in that separate readings are made at each gage. During the calibration process it became apparent that several gages were not functioning. In these instances, only a single gage was used to determine strain and stress at that particular location.

LOAD TEST RESULTS

Moment

The moments were calculated at each strain gage pair location. The moment distributions along the pile length at the beginning, middle, and end of each time interval for Tests 1, 2, and 3 are shown in Figures 11 - 19. After applying the maximum load of 266.7 pounds, the pile was unloaded. Measurements were also made during the unloading. The unloading was done in three equal increments. The legend on the figures indicates the magnitude of the applied lateral load. Increasing loads are shown as “UP” and the unloading is indicated by “DOWN.” The moment curves show a logical smooth moment distribution

along the pile length with the only discontinuity showing up at gage location 10. The results from the gage pair at location 10 are not included in the following figures. The results show a smoother distribution of moment.

For clarity, Figure 20 is a graph of Test 1, moment versus load at the minimum applied load of 41.6 pounds, a mid load of 146.9 pounds, and the maximum load of 266.7 pounds. The results show the point of fixity advancing down the pile as the load is increased. The pile undergoes a moment reversal (contraflexure) for the minimum and mid loads. The maximum load causes “short pile” behavior and the pile is no longer fixed at its base.

Pile Top Deflection

Pile top deflection and slope was measured by means of linear variable differential transformers (LVDT's) during load Tests 4, 5, and 6. The deflection was measured at the location of the applied lateral force. A second LVDT, positioned 810mm above the first LVDT, measured deflection at that point on the pile. The ratio of the distance between measurements to the difference in deflection provides the slope of the pile at the point of load application. A plot of pile top deflection and pile top slope versus applied lateral load is shown in Figures 21 and 22 respectively.

p-y Curves

The most widely used analysis technique for evaluating the nonlinear response of laterally loaded piles is the p-y method, where p is the soil resistance per unit length of pile and y is the lateral soil or pile deflection. The p-y relationship was determined at each strain gage location in the soil profile by means of the familiar relationship:

where : M = moment

I = moment of inertia of pile

y = pile deflection

x = location along pile axis (ie depth)

A best fit curve was established for each moment curve for each load increment from Test 1. These curves, along with the associated polynomial expression, are shown in Figures 23-30. The curves were integrated commencing from the bottom and working up the pile length to establish the change in pile slope from point to point. The procedure was repeated and the pile slopes were integrated, commencing at the pile bottom and working up the pile length to establish the change in pile deflection from point to point. The boundary conditions employed were that both slope and deflection were assumed to be zero at the pile tip. The integration was not performed on the moment curve corresponding to the

$$\frac{M}{E I} = \frac{d^2 y}{dx^2}$$

maximum load since it appears that the boundary conditions may not be valid (ie. the slope does not appear to be zero).

The polynomial was differentiated twice at each point along the pile length in order to get the “p” portion of the p-y curves. Since this involved evaluating pile slopes and changes in slope, it was essential that the polynomial matched the curvature of the moment curve as closely as possible. This operation was more critical than the integration since measurement errors can incorrectly imply curvature of the pile. One point on a p-y curve was determined at each strain gage location for each moment curve. A typical calculated p-y curve is shown in Figure 31. The development of the p-y curves was not completely

successful and the “typical” curve shape assumed in most lateral load analyses was not duplicated. Further work with the curve fittings is necessary and is being pursued.

Measured versus Predicted Behavior

The predicted pile behavior using both the LPGSTAN and COM624P computer programs was compared to the model results. The undrained shear strength of the clay soil in the test cell was measured immediately after each of the six tests at both cell locations. A miniature vane shear apparatus was used and the results are shown in Figures 32 and 33. The undrained shear strength profile was used as input data for the computer programs. Analyses were made using both the actual strength profile and an average strength profile.

Pile Moment

The measured moments from Tests 1, 2, and 3 closely matched the predicted results from both the LPGSTAN and COM624P computer programs. Moment comparisons from Test 1 for minimum, mid, and maximum lateral loads are shown in Figures 34-37. The maximum moment as well as the location of maximum moment are in good agreement. Also the measured points of reverse curvature (contra-flexure) closely coincide with the predicted results.

Pile Top Movement

The measured pile top deflection versus lateral load for Test 4 is compared with the predicted movements from LPGSTAN and COM624P in Figure 38. The predicted deflections compare fairly well with the measured values particularly for applied loads not exceeding 225 pounds. At that load, the model pile top deflected 1.25 inches. This corresponds to a prototype movement of over 12 inches due to a lateral load of approximately 22.5 kips.

CONCLUSIONS

The purpose of Phase I was to develop an model pile test facility and instrumentation/monitoring program. To that end, Phase 1 was very successful. A model test facility and a reliable testing, instrumentation, and data collection procedure has been developed. The LPGSTAN computer model was verified for a single pile subjected to lateral loading. The experience gained from the Phase 1 portion of this program will be invaluable as the issues of group effects and cyclic loading are pursued in the subsequent phases of this ongoing research.

REFERENCES

McVay, M.C., Development of a Coupled Bridge and Superstructure Foundation Finite Element Code.
Final Report to Florida Department of Transportation, State Job No. 99700-7564010, Contract
B-8415, June 1993.

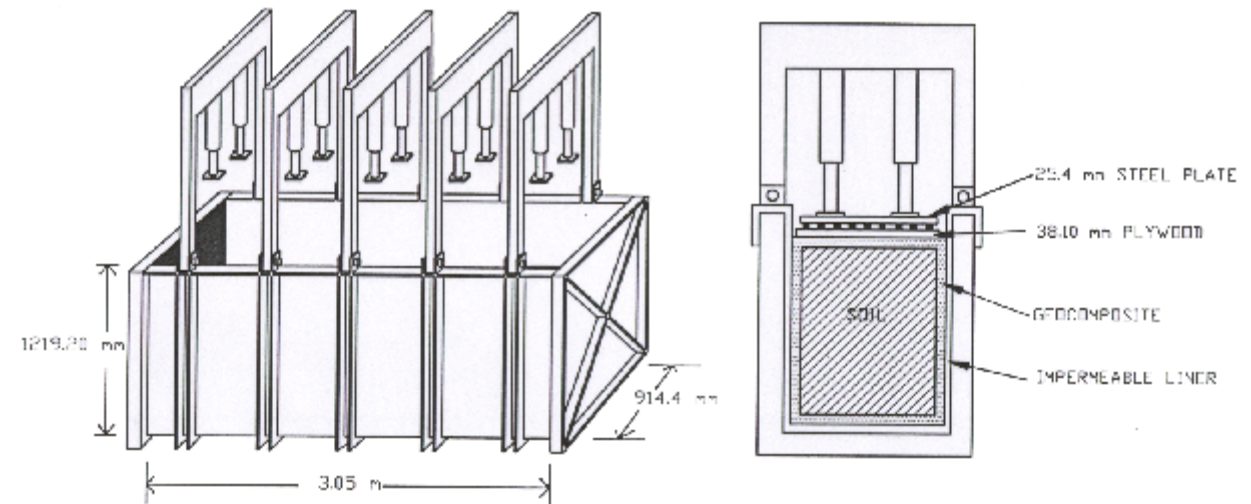
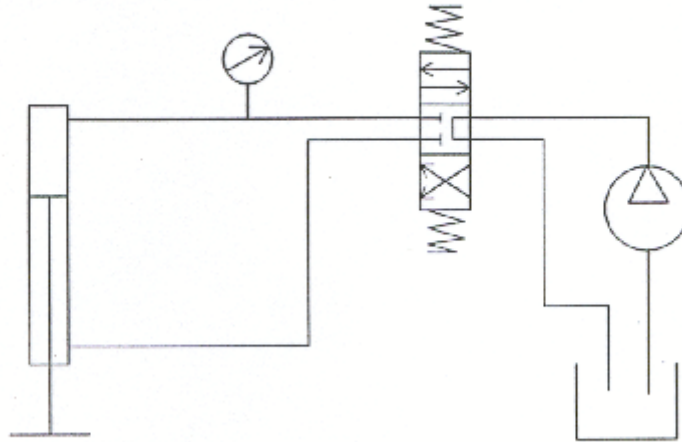


Figure 1. Utah State University Model Test Facility

Simplified Hydraulic Schematics

Before Hydraulic Accumulator



With Hydraulic Accumulator

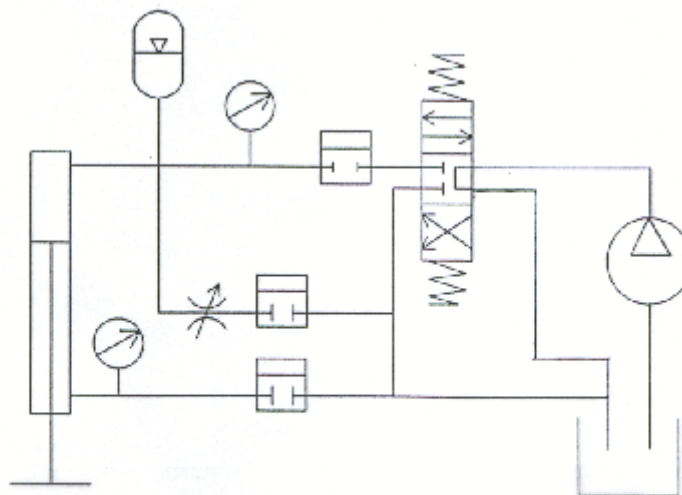


Figure 2. Simplified Hydraulic Schematic

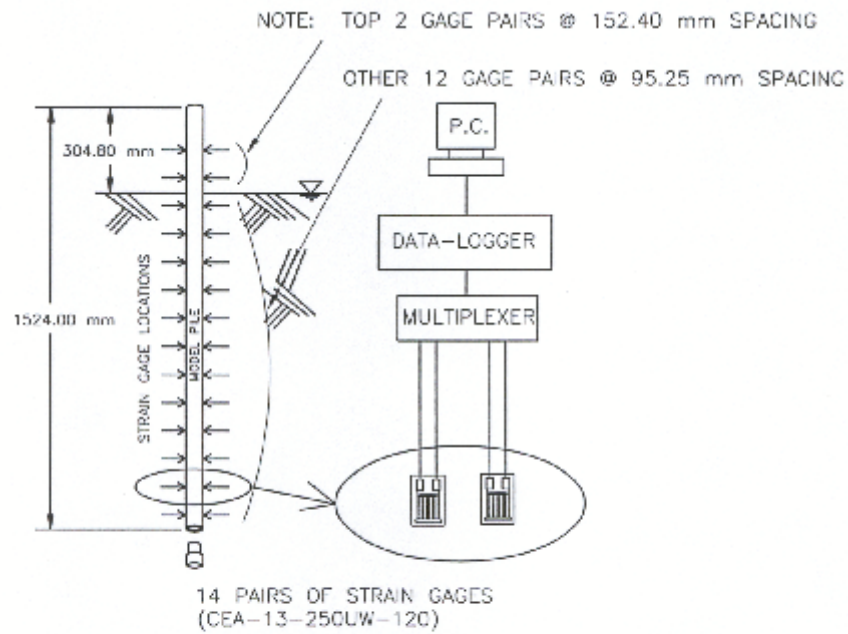


Figure 3. Model Pile and Strain Gage Locations

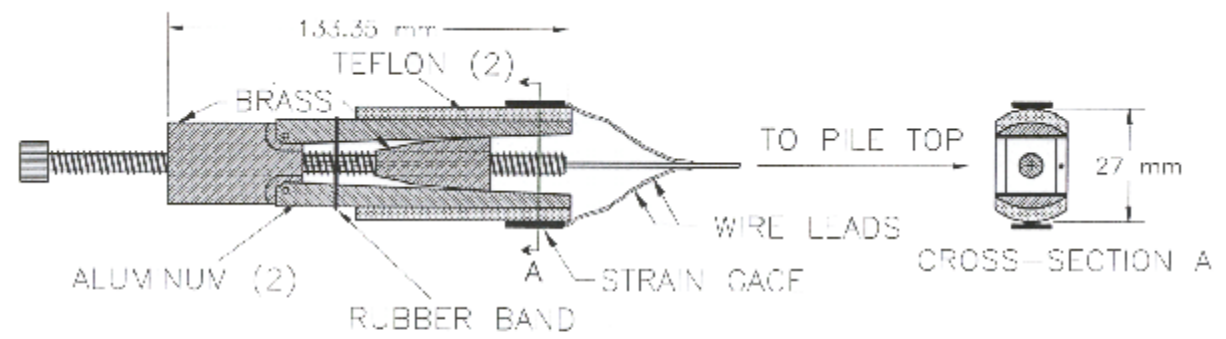


Figure 4. Utah State University Strain Gage Installation Tool

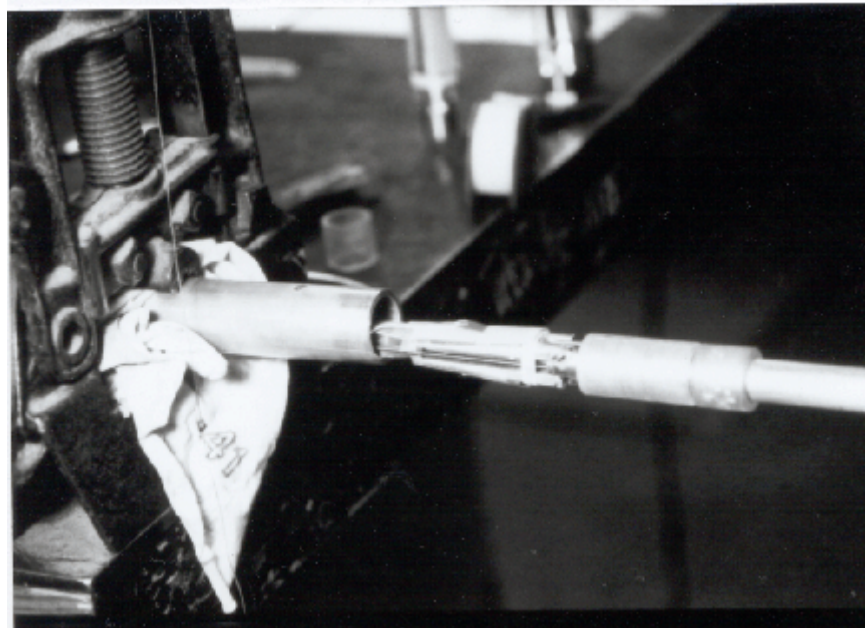
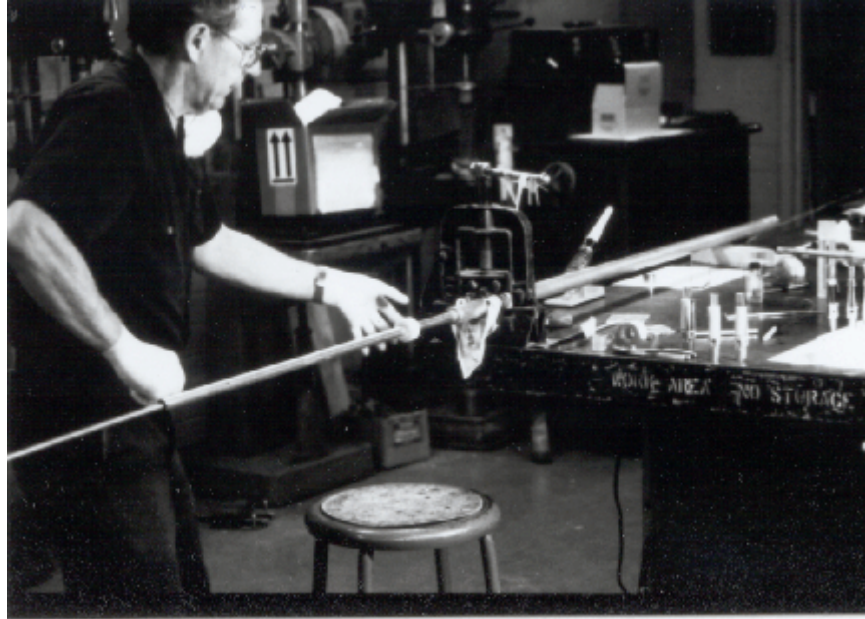


Figure 5. Photographs Showing Strain Gage Installation

TEMPERATURE-COMPENSATED QUARTER-BRIDGE

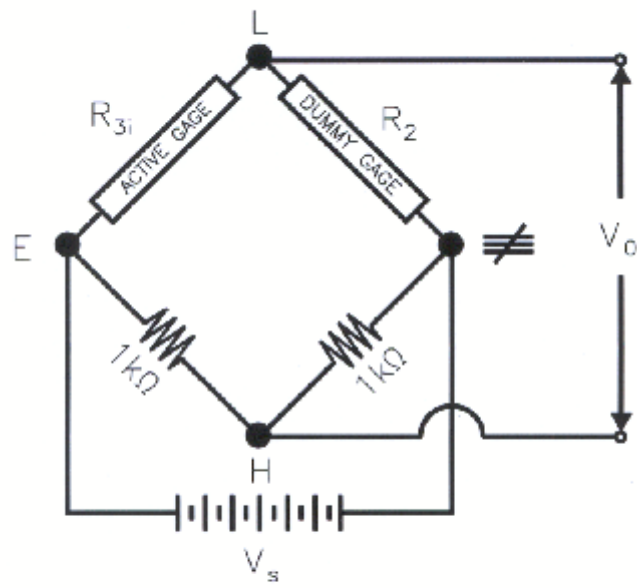


Figure 6. Wheatstone Bridge

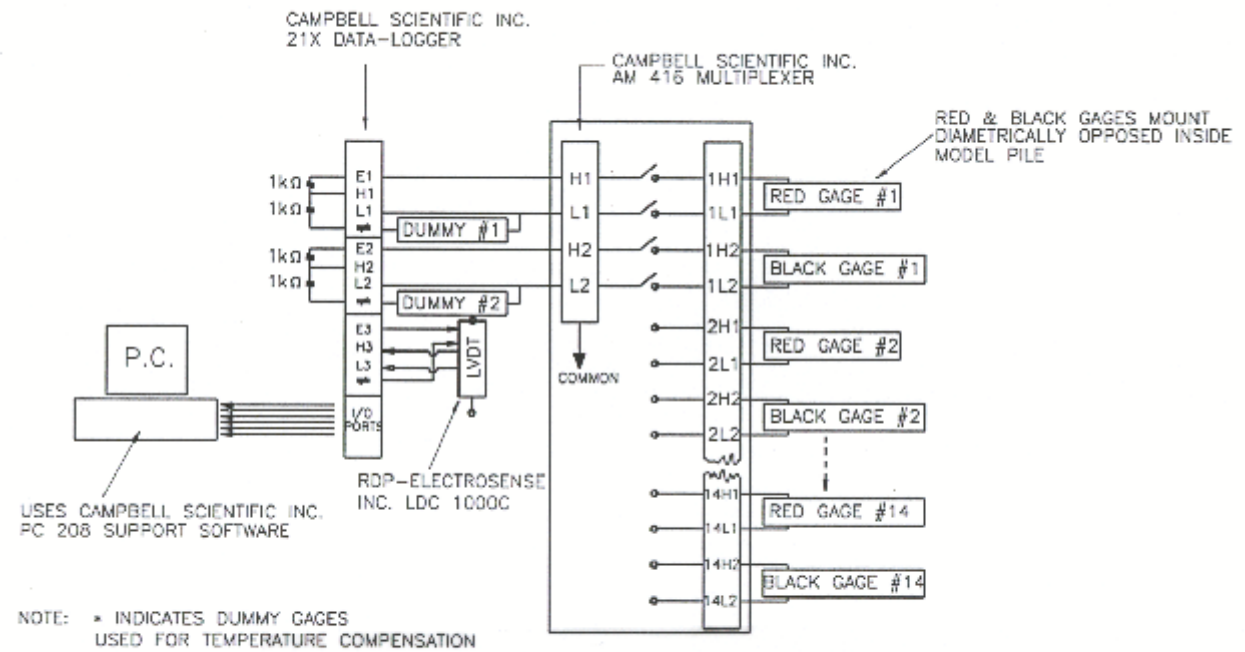
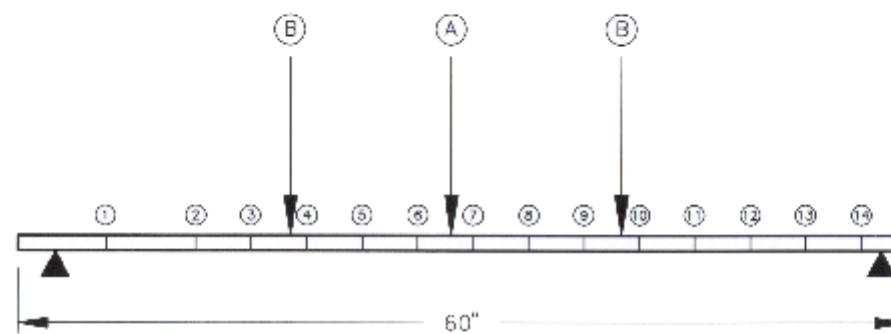


Figure 7. Data Acquisition System

STRAIN GAGE LOCATIONS AND CALIBRATION LOADS



- Notes:
- Both load cases ranged between 0 and 253 lbs.
 - The associated stresses were approximately 70% of the yield stresses for both cases

Two Loading Configurations for Calibration

- (A) - Concentrated Loads @ Center
- (B) - Two Concentrated Loads equidistant from supports

Figure 8. Calibration Loadings

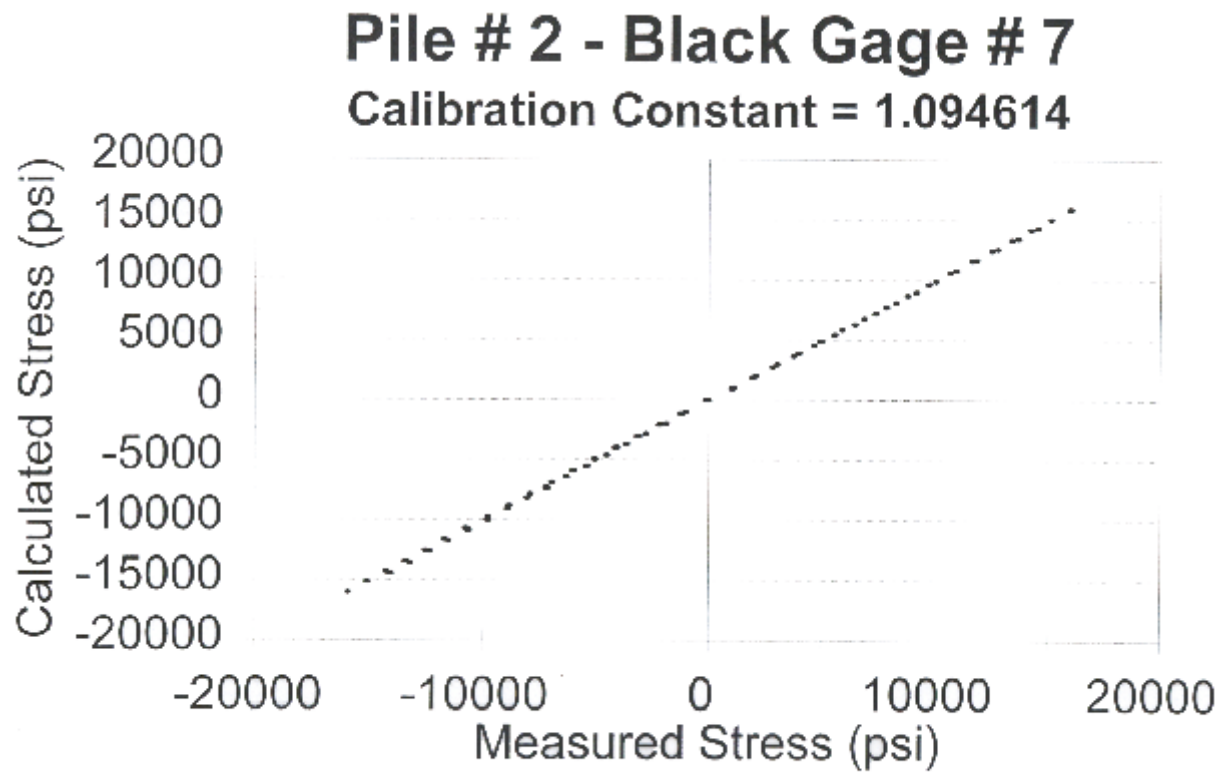


Figure 9. Calibration Curve, Strain Gage #7, Black

Pile # 2 - Red Gage # 7
Calibration Constant = 1.380346

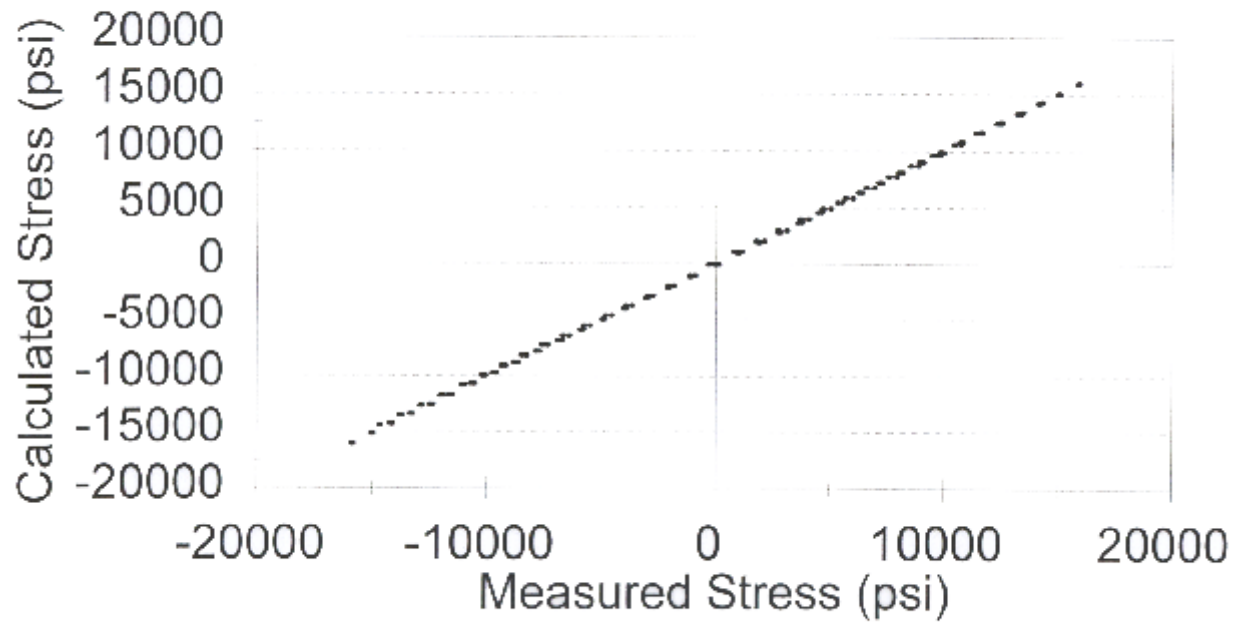


Figure 10. Calibration Curve, Strain Gage #7, Red

Moment Profile : Test # 1

Beginning of Time Interval

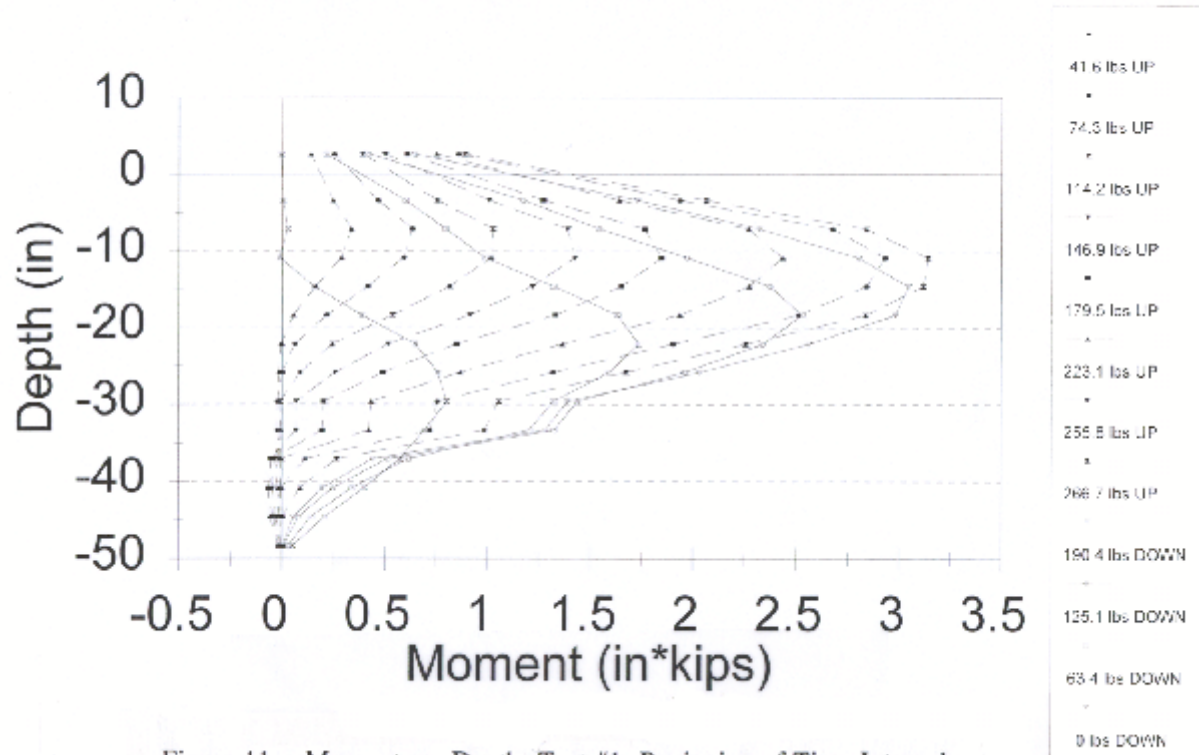


Figure 11. Moment vs. Depth, Test #1, Beginning of Time Interval

Moment Profile : Pile Test # 1

Midpoint of Time Interval

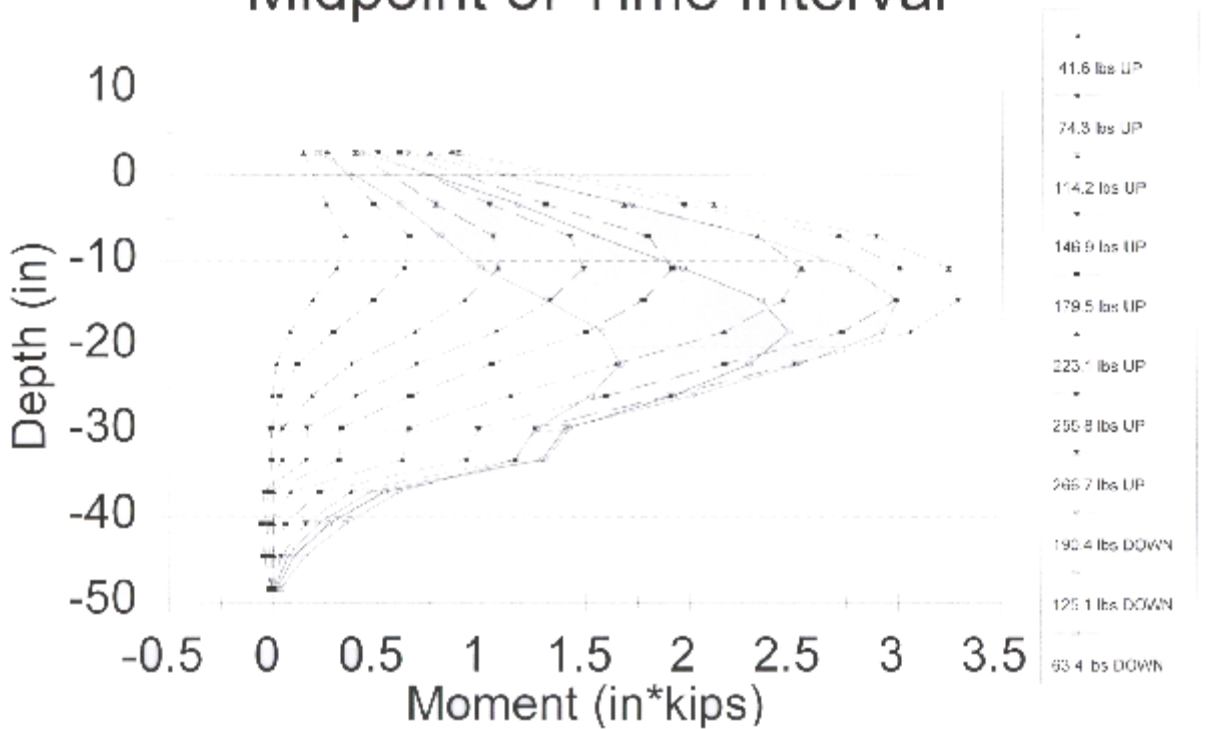


Figure 12. Moment vs. Depth, Test #1, Middle of Time Interval

Moment Profile : Pile Test # 1

End of Time Interval

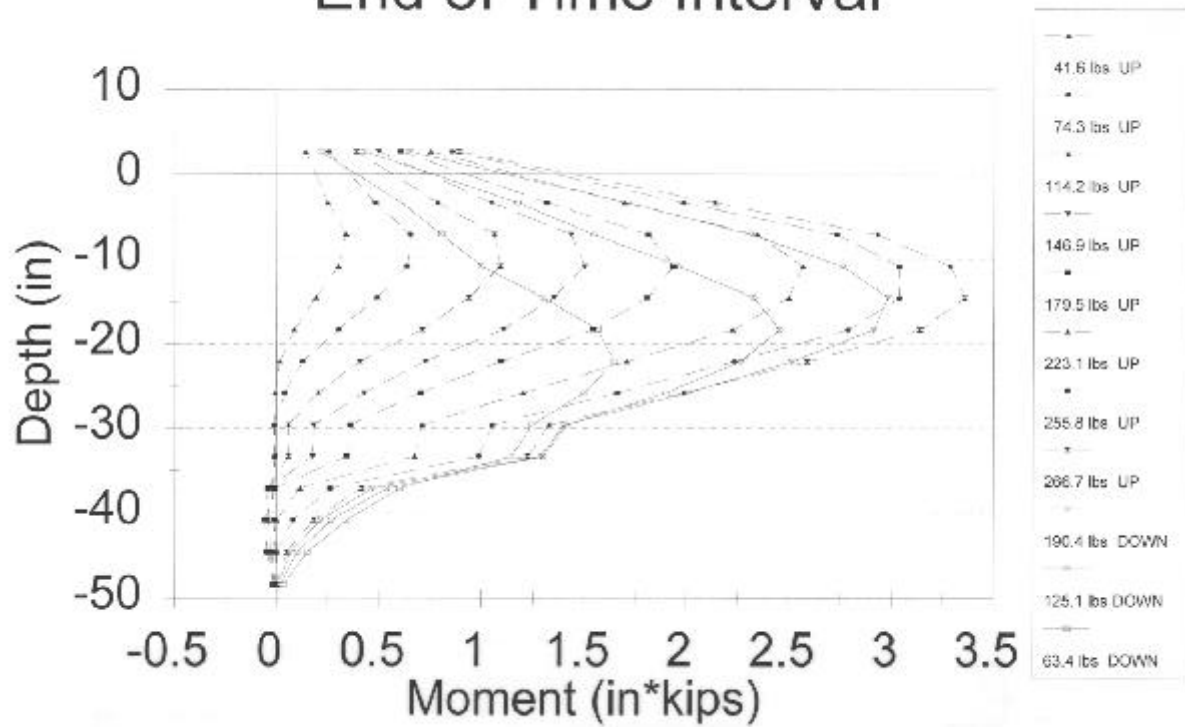


Figure 13. Moment vs. Depth, Test #1, End of Time Interval

Moment Profile : Test #2

Beginning of Time Interval

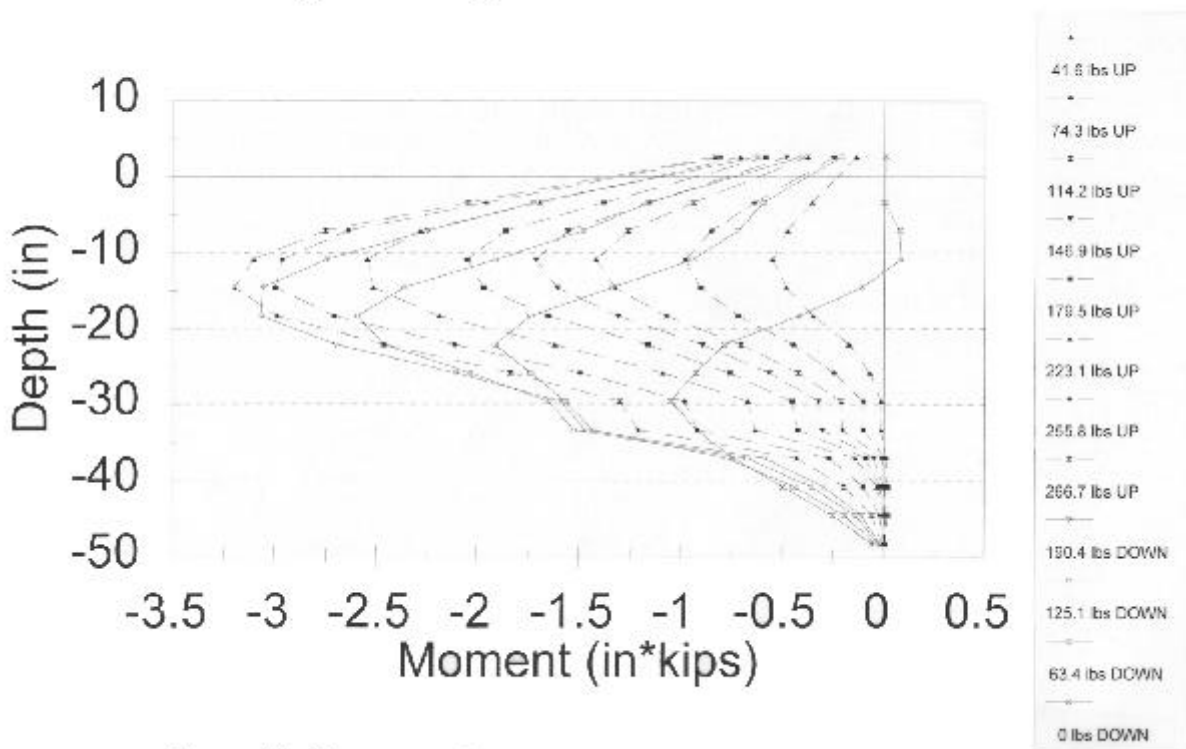


Figure 14. Moment vs. Depth, Test #2, Beginning of Time Interval

Moment Profile : Pile Test #2

Midpoint of Time Interval

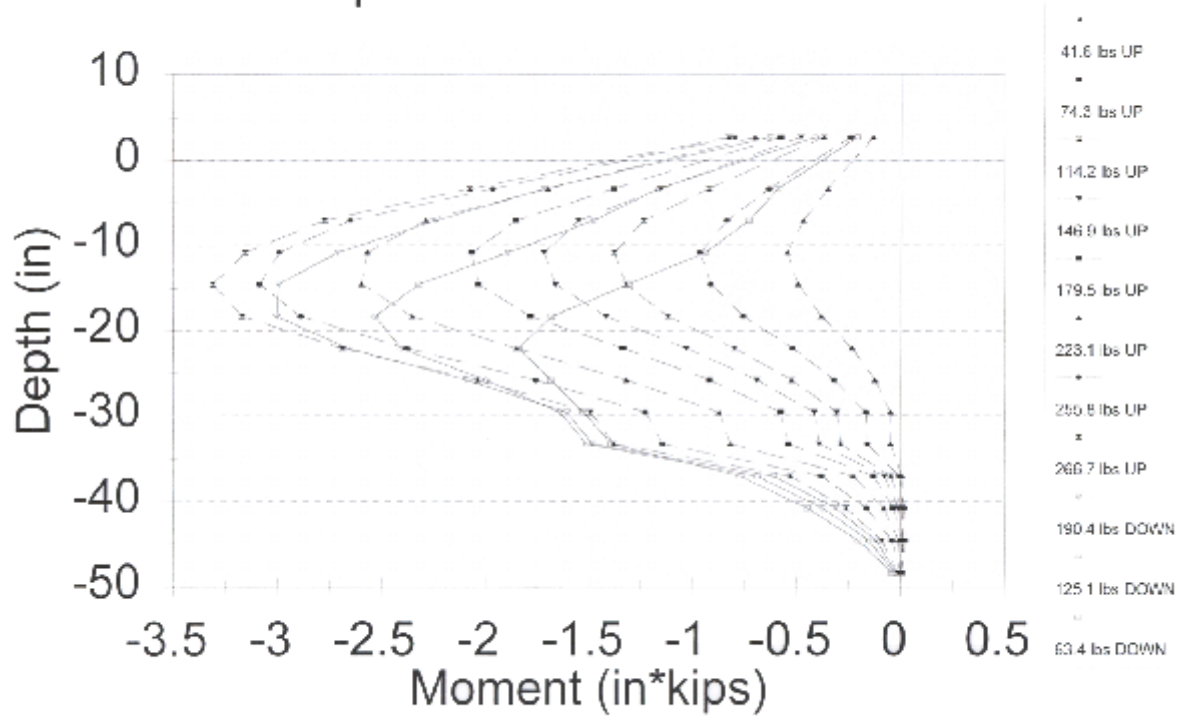


Figure 15. Moment vs. Depth, Test #2, Middle of Time Interval

Moment Profile : Pile Test #2

End of Time Interval

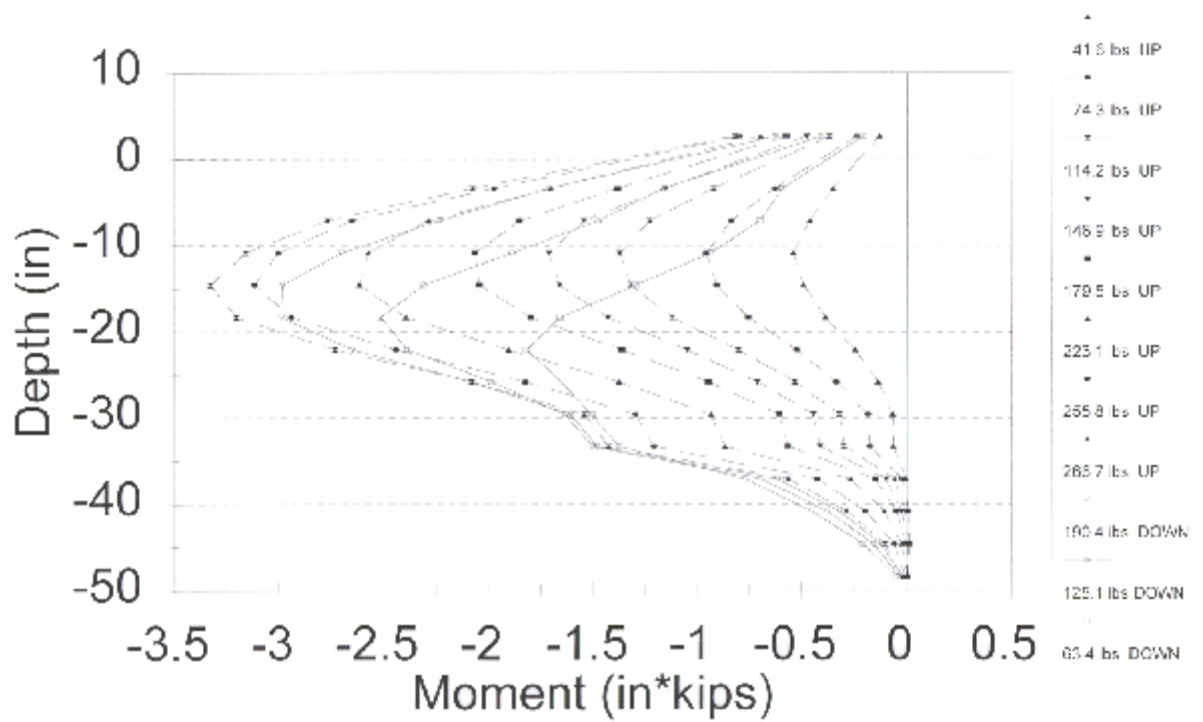


Figure 16. Moment vs. Depth, Test #2, End of Time Interval

Moment Profile : Test #3

Beginning of Time Interval

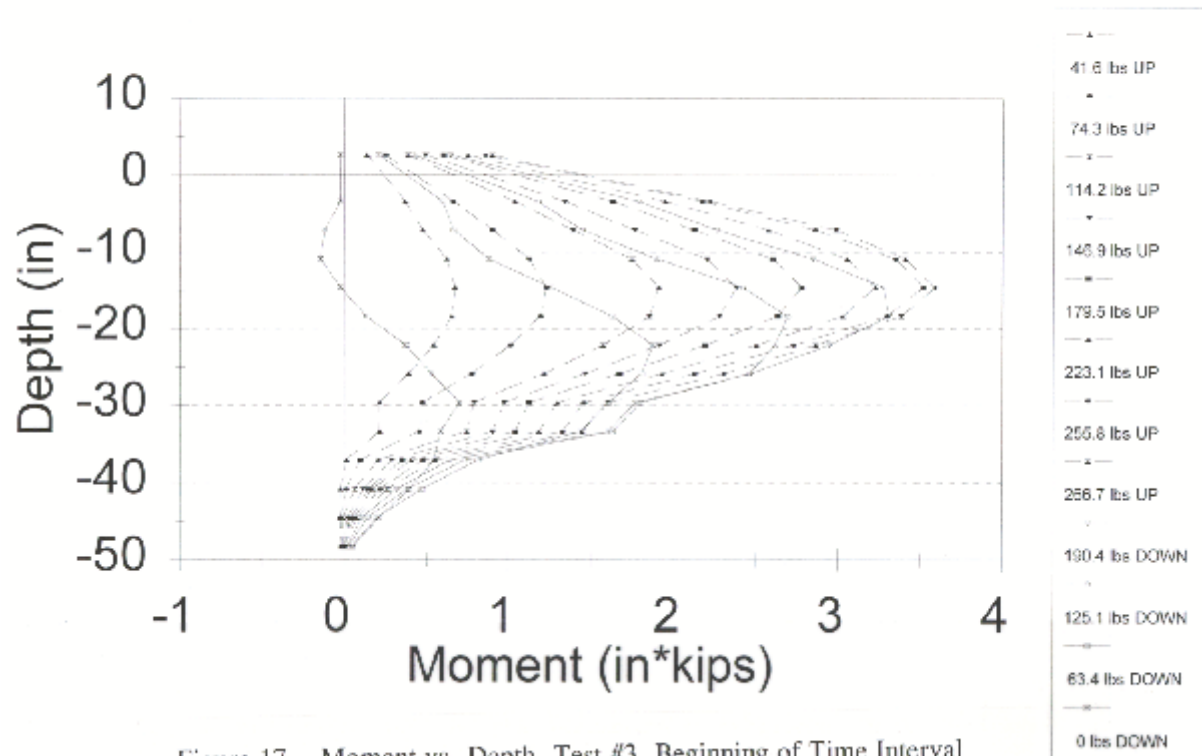


Figure 17. Moment vs. Depth, Test #3, Beginning of Time Interval

Moment Profile : Pile Test #3

Midpoint of Time Interval

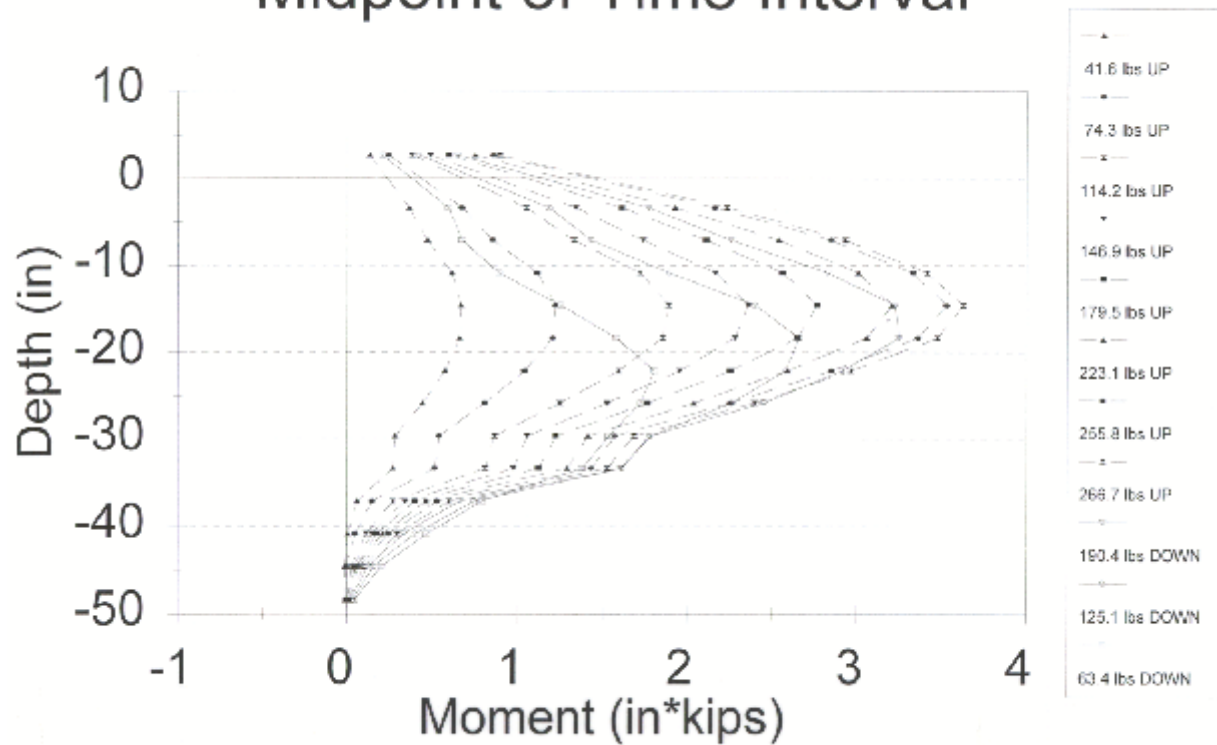


Figure 18. Moment vs. Depth, Test #3, Middle of Time Interval

Moment Profile : Pile Test #3

End of Time Interval

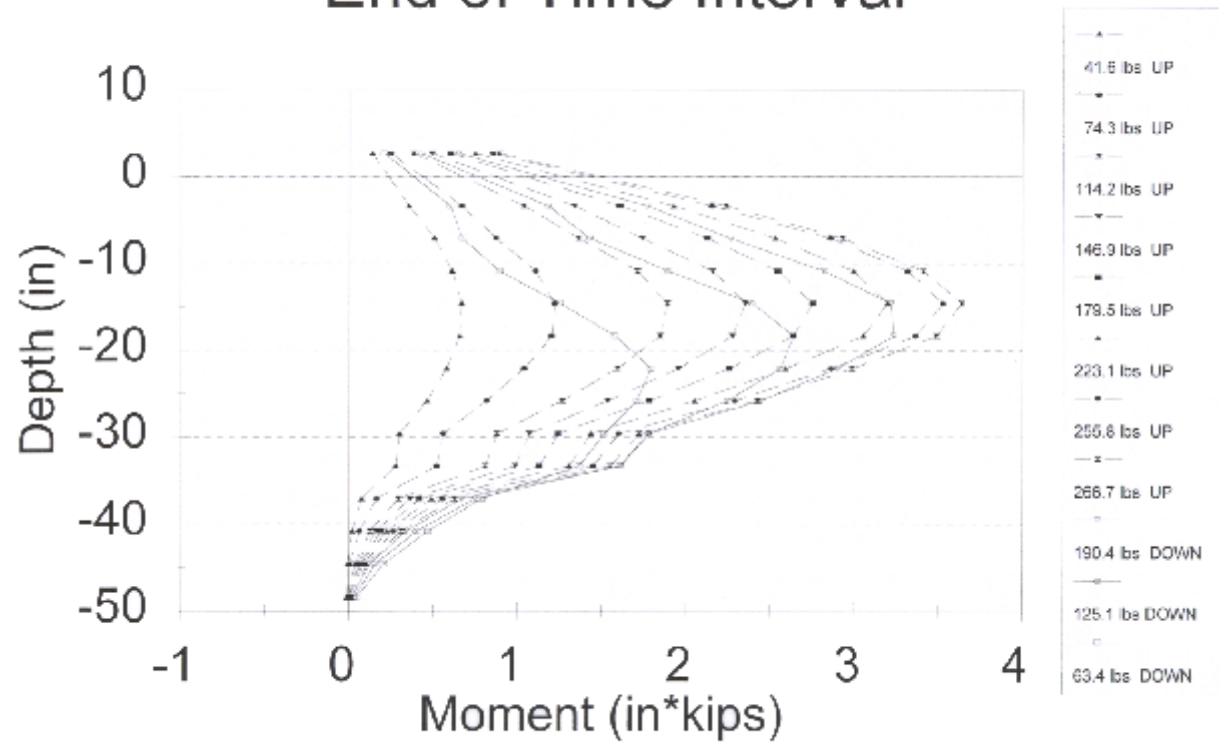


Figure 19. Moment vs. Depth, Test #3, End of Time Interval

Moment Profiles : Test #1

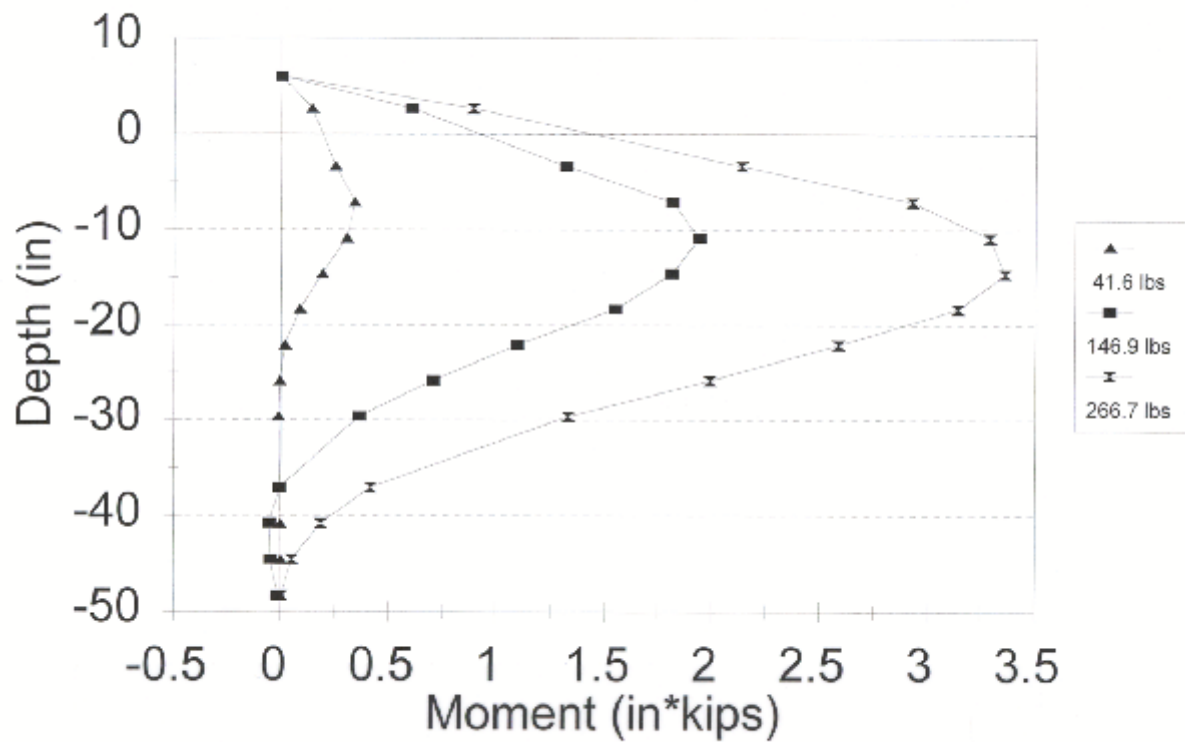


Figure 20. Moment vs. Depth, Test #1, End of Time Interval
Minimum, Mid Range, and Maximum Lateral Load

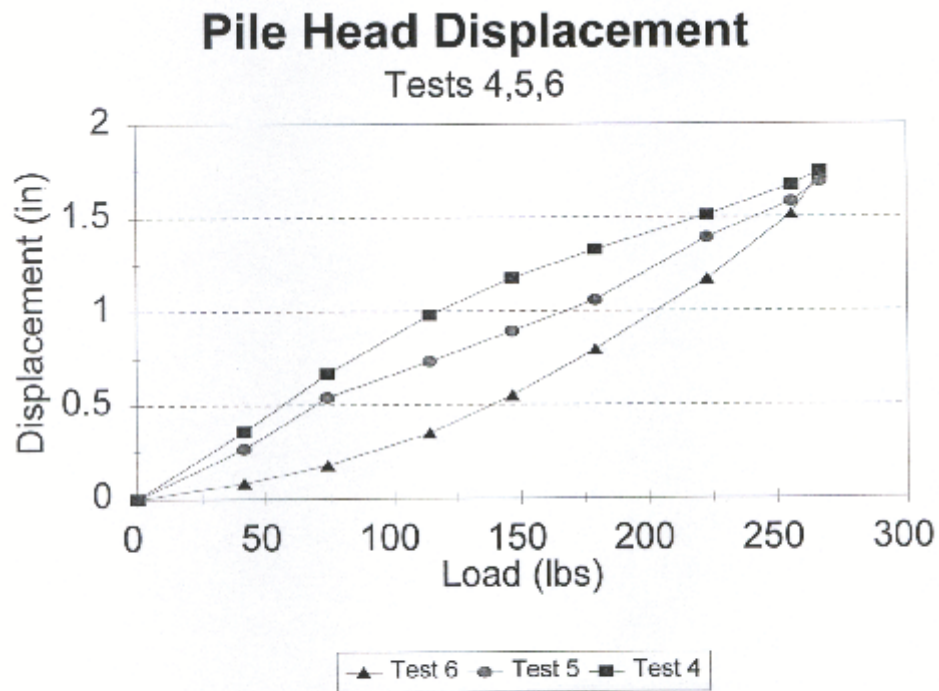


Figure 21. Measured Pile Top Displacement vs. Applied Lateral Loads, Tests 4, 5 , & 6

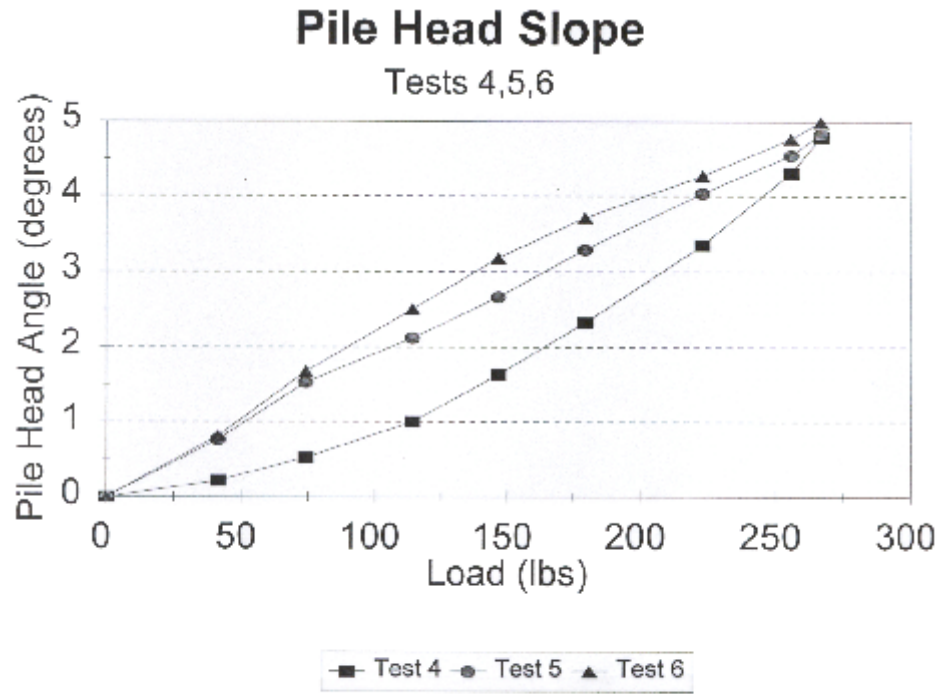


Figure 22. Measured Pile Top Slope vs. Applied Lateral Loads, Tests 4, 5, & 6

41.6 lbs. lateral force

Rank 2 Eqn 7008 $y=(a+cx+ex^2+gx^3+ix^4)/(1+bx+dx^2+fx^3+hx^4+jx^5)$

$r^2=0.99789501$ DF Adj $r^2=0.99087839$ FitStdErr=0.010519409 Fstat=210.69444

$a=0.18266572$ $b=0.019671675$ $c=-0.014946857$ $d=-0.011924926$ $e=-0.0021495235$

$f=-0.0012849645$ $g=-6.5407464e-05$ $h=-4.0562216e-05$ $i=-5.981676e-07$ $j=-4.2106357e-07$

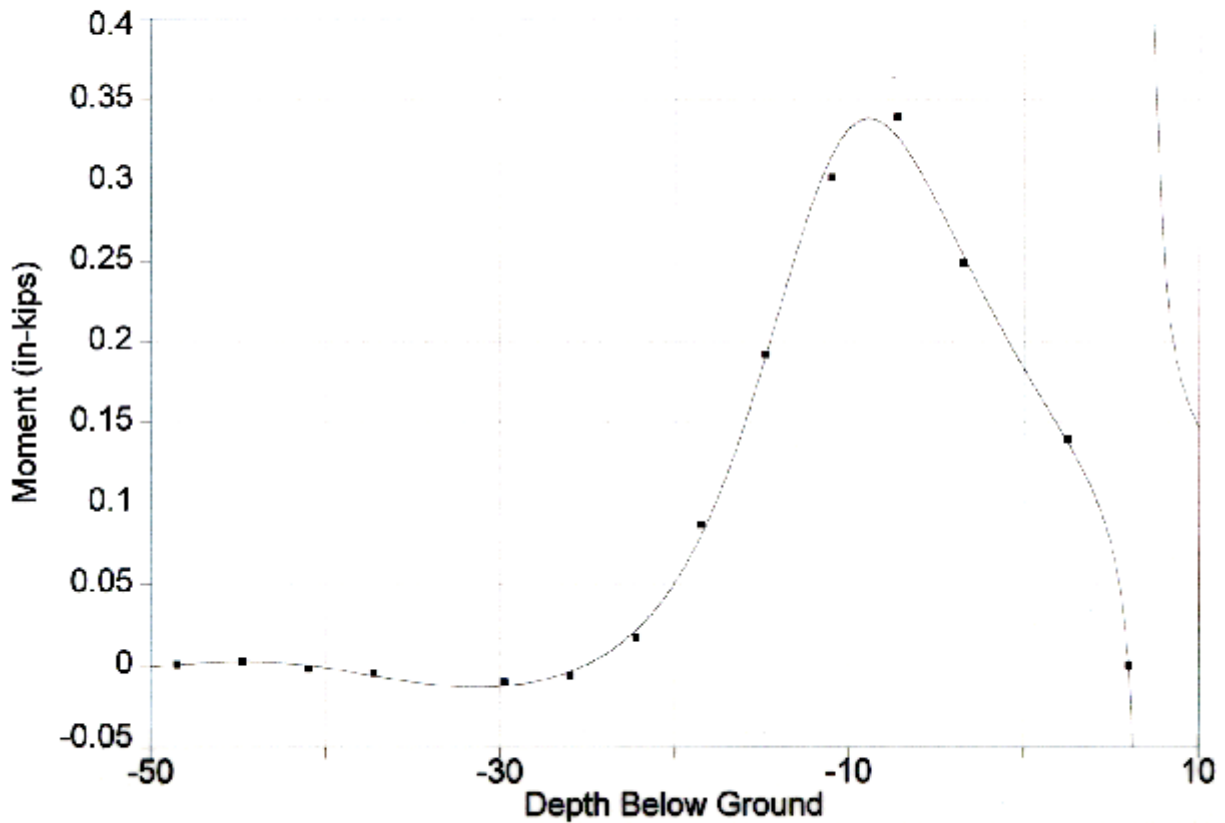


Figure 23. Best Fit Polynomial for Moment Distribution, Lateral Load, 41.6 lbs

74.3 lbs lateral force

Rank 7 Eqn 7006 $y=(a+cx+ex^2+gx^3)/(1+bx+dx^2+fx^3+hx^4)$

$r^2=0.99682314$ DF Adj $r^2=0.99174016$ FitStdErr=0.021361119 Fstat=268.95083

$a=0.36343286$ $b=0.019752842$ $c=-0.039425803$ $d=-0.0015530017$

$e=-0.0030097746$ $f=-9.3386819e-05$ $g=-4.1964969e-05$ $h=3.3876059e-06$

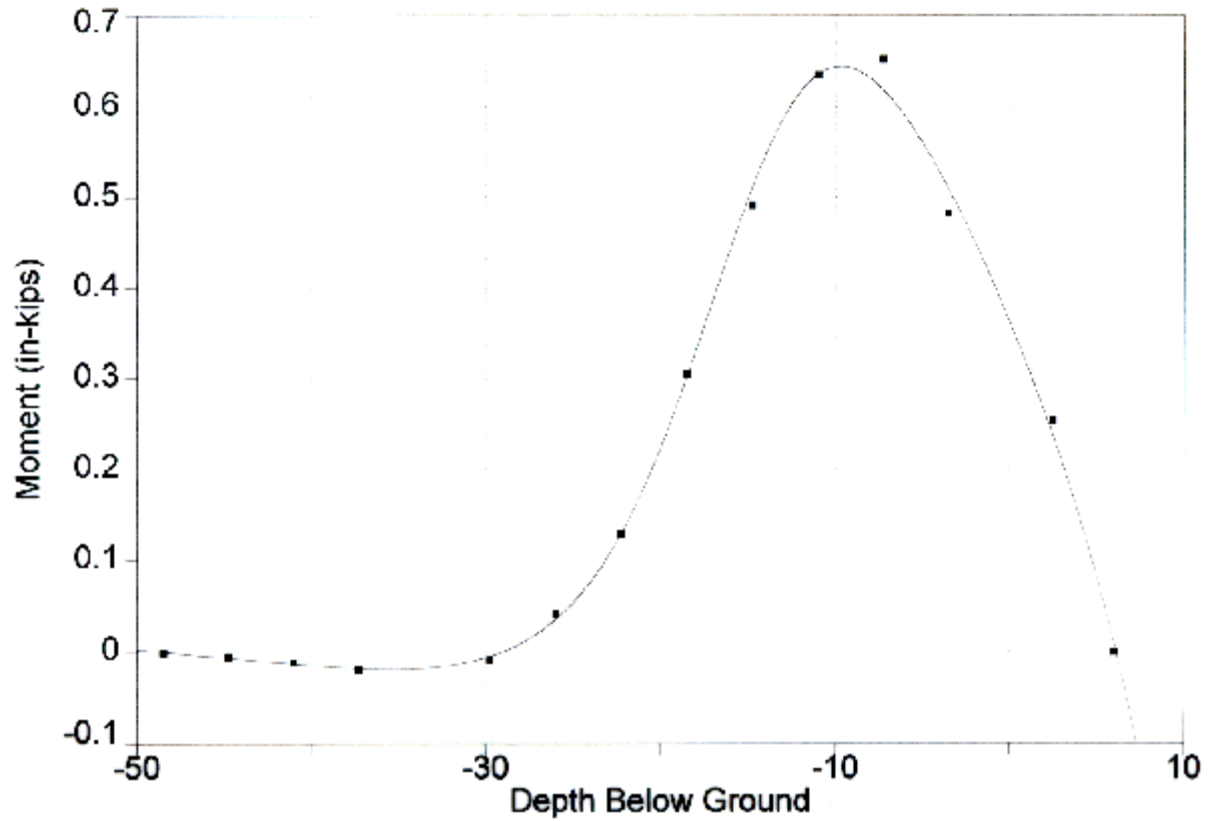


Figure 24. Best Fit Polynomial for Moment Distribution, Lateral Load, 74.3 lbs

114.2 lbs lateral force

Rank 7 Eqn 7005 $y=(a+cx+ex^2+gx^3)/(1+bx+dx^2+fx^3)$

$r^2=0.99774403$ DF Adj $r^2=0.99511206$ FitStdErr=0.028399128 Fstat=615.9/94

a=0.5775633 b=0.025747819 c=-0.065431689 d=-0.00048910234

e=-0.0044868948 f=-8.4544193e-05 g=-5.9319553e-05

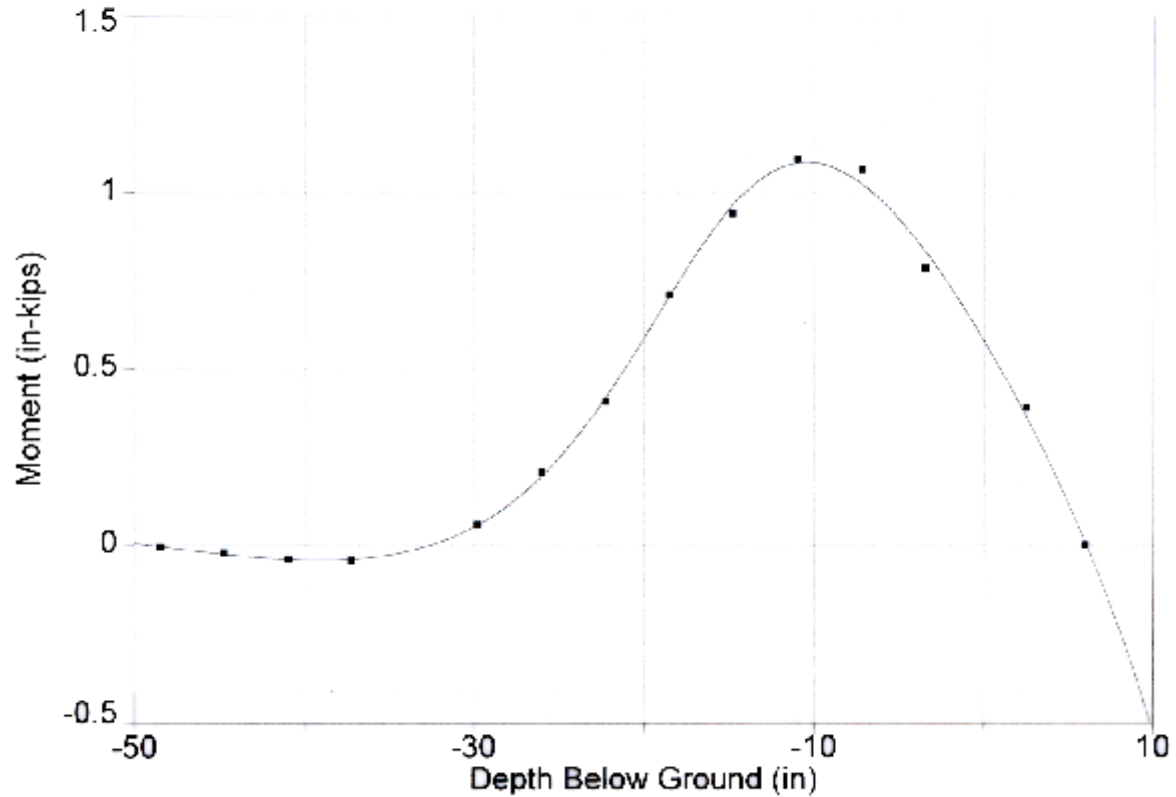


Figure 25. Best Fit Polynomial for Moment Distribution, Lateral Load, 114.2 lbs

146.9 lbs lateral force

Rank 5 Eqn 7005 $y=(a+cx+ex^2+gx^3)/(1+bx+dx^2+fx^3)$

$r^2=0.99792794$ DF Adj $r^2=0.99551054$ FitStdErr=0.037496523 Fstat=561.8805

$a=0.75666198$ $b=0.031772213$ $c=-0.087395825$ $d=0.00049973334$

$e=-0.0056268612$ $f=-3.7423613e-05$ $g=-7.1785067e-05$

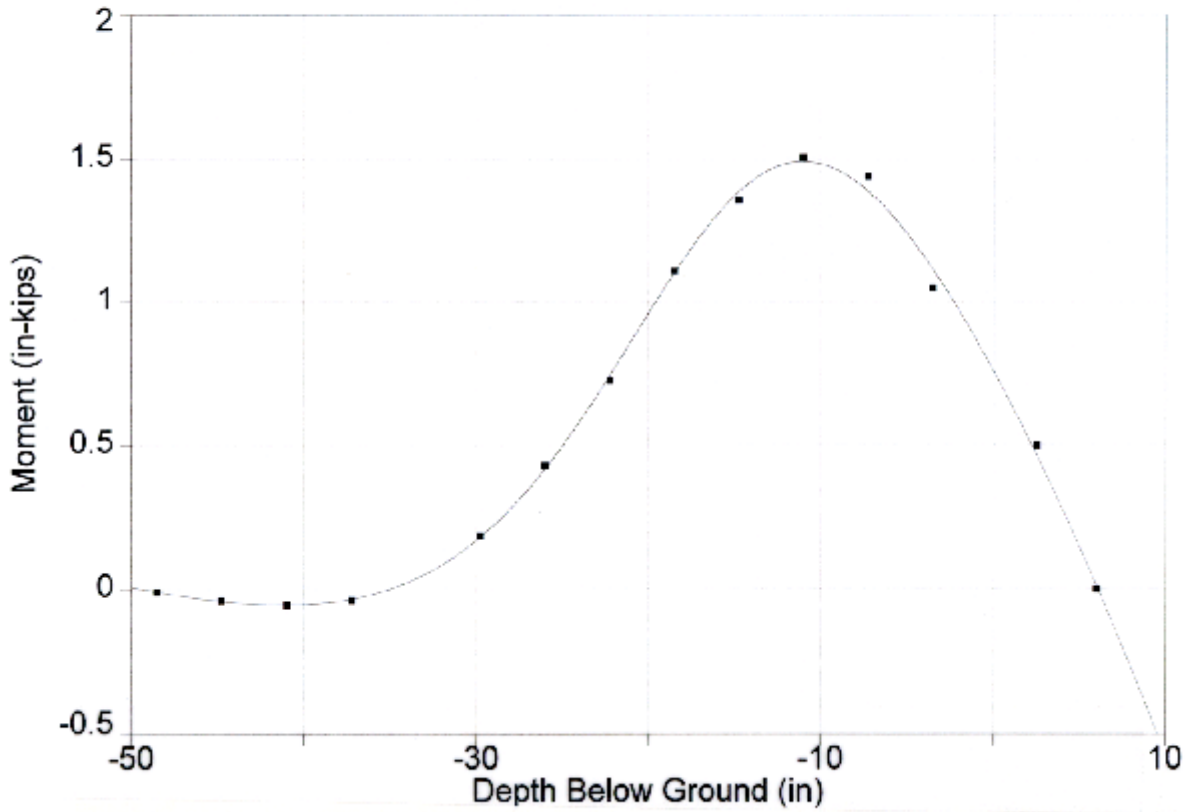


Figure 26. Best Fit Polynomial for Moment Distribution, Lateral Load, 146.9 lbs

179.5 lbs lateral force

Rank 4 Eqn 7005 $y=(a+cx+ex^2+gx^3)/(1+bx+dx^2+fx^3)$

$r^2=0.99846178$ DF Adj $r^2=0.99666719$ FitStdErr=0.041649183 Fstat=757.28526

a=0.93707164 b=0.033433807 c=-0.11011507 d=0.00073463668

e=-0.0067432144 f=-2.2676791e-05 g=-8.3569694e-05

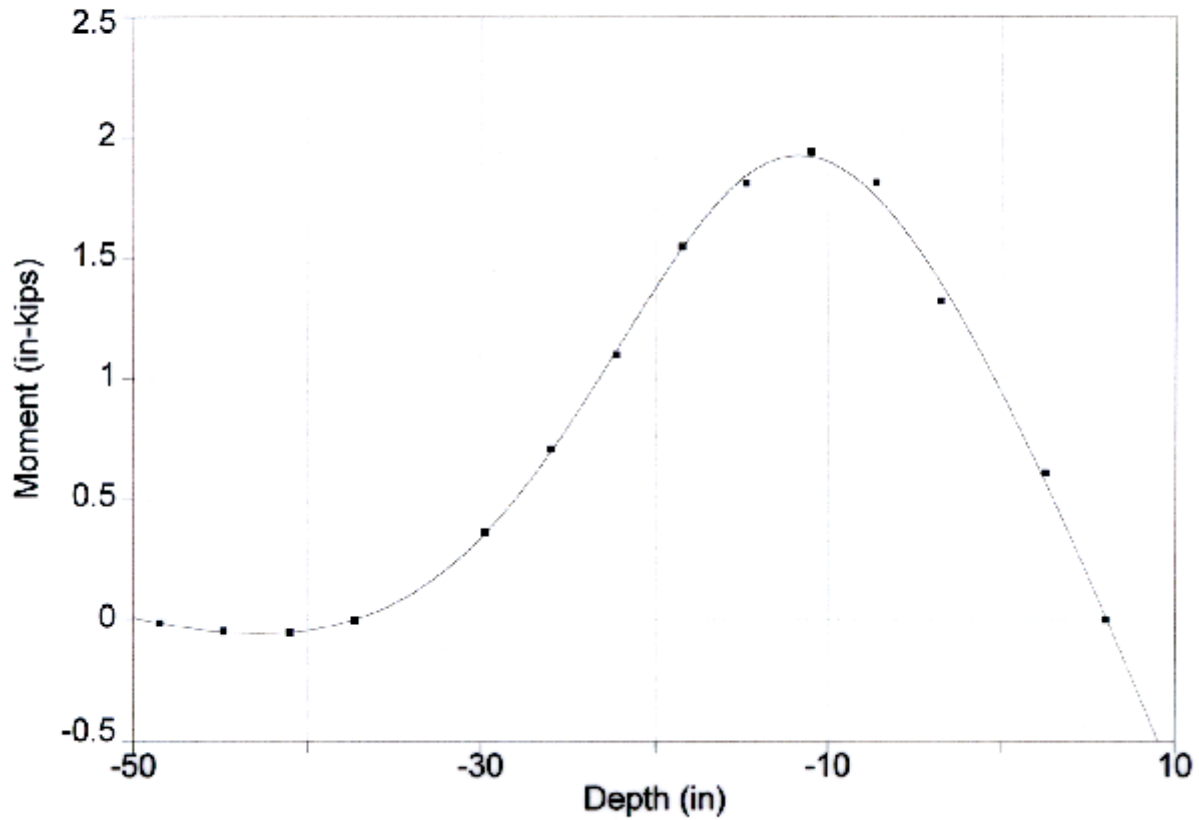


Figure 27. Best Fit Polynomial for Moment Distribution, Lateral Load, 179.5 lbs

223.1 lbs lateral force

Rank 6 Eqn 7005 $y=(a+cx+ex^2+gx^3)/(1+bx+dx^2+fx^3)$

$r^2=0.99892895$ DF Adj $r^2=0.99767938$ FitStdErr=0.046001555 Fstat=1068.1027

a=1.1840911 b=0.034238989 c=-0.14239513 d=0.0008524179

e=-0.0081255643 f=-1.3039236e-05 g=-9.6326177e-05

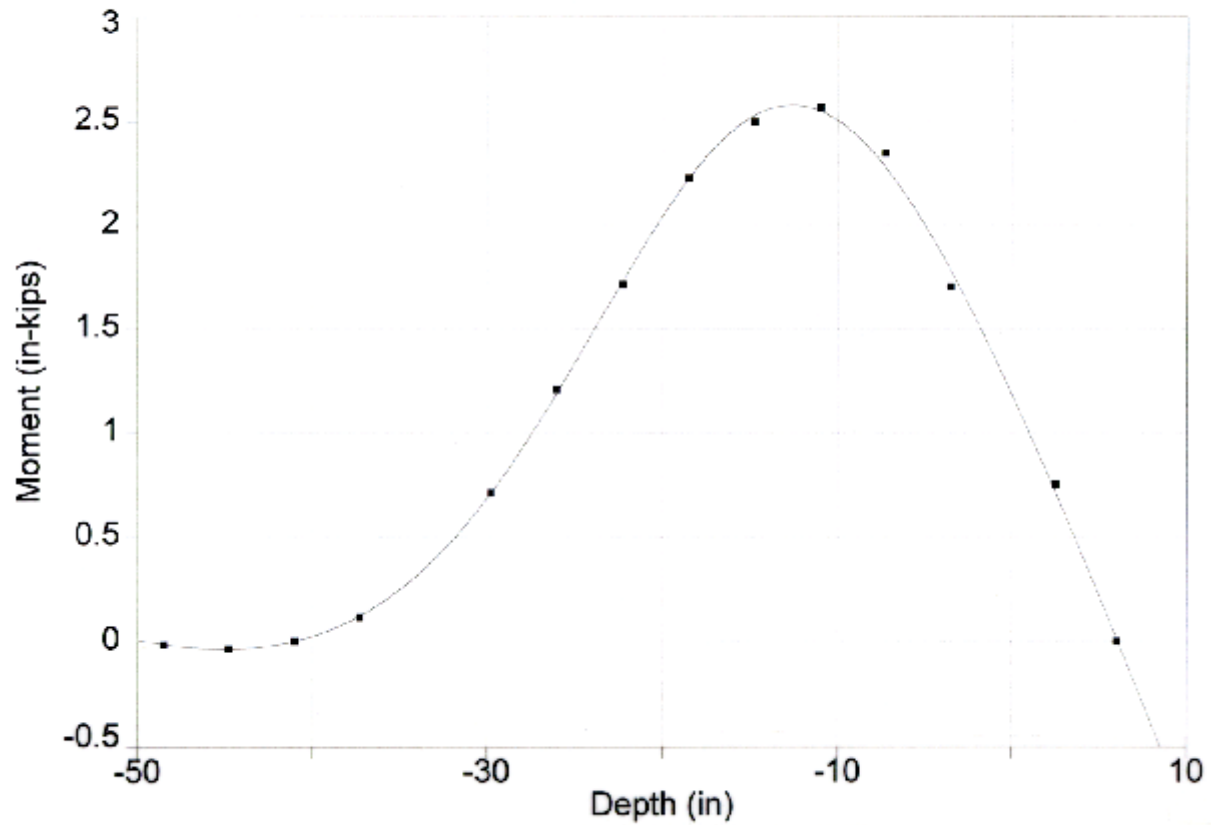


Figure 28. Best Fit Polynomial for Moment Distribution, Lateral Load, 223.1 lbs

255.8 lbs lateral force

Rank 5 Eqn 7005 $y=(a+cx+ex^2+gx^3)/(1+bx+dx^2+fx^3)$

$r^2=0.99925847$ DF Adj $r^2=0.99839335$ FitStdErr=0.045428878 Fstat=1572.1588

a=1.3673218 b=0.03317511 c=-0.16742768 d=0.00079230743

e=-0.0090258723 f=-1.1231316e-05 g=-0.00010279016

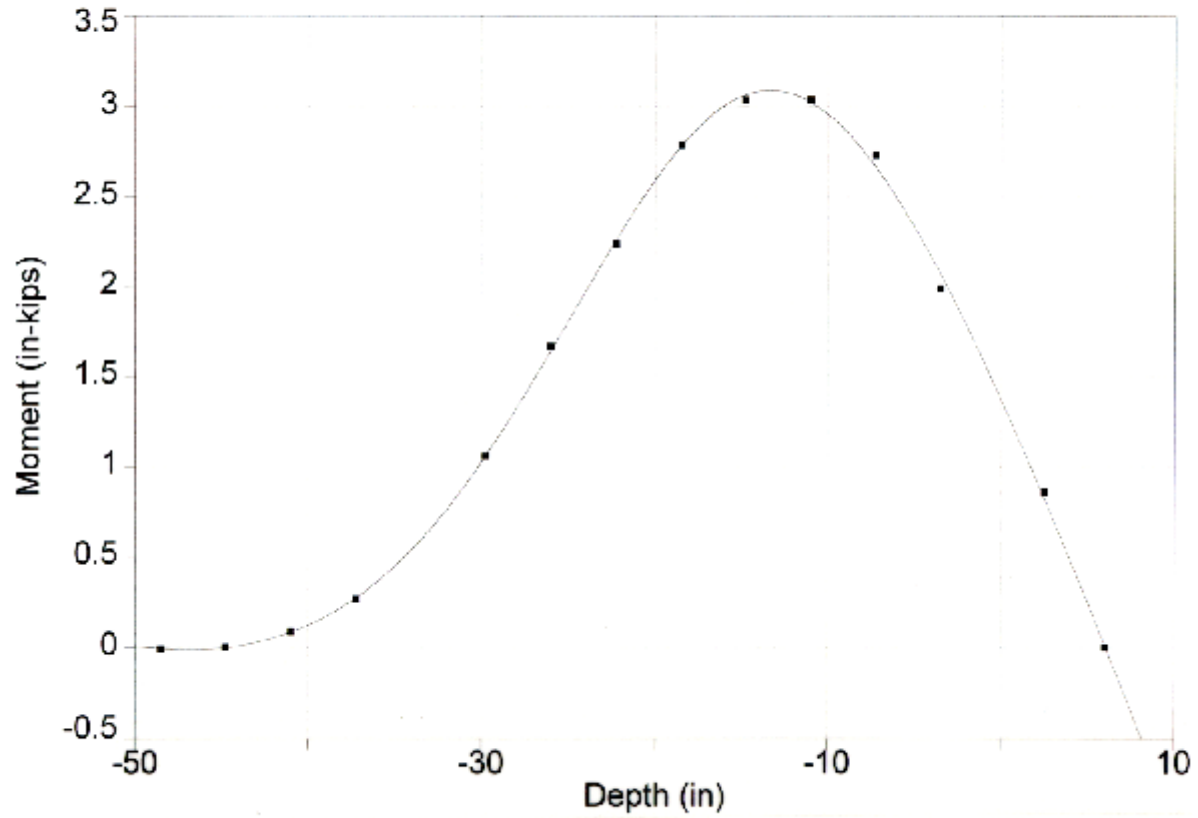


Figure 29. Best Fit Polynomial for Moment Distribution, Lateral Load, 255.8 lbs

266.7 lbs lateral force

Rank 4 Eqn 7005 $y=(a+cx+ex^2+gx^3)/(1+bx+dx^2+fx^3)$

$r^2=0.99953121$ DF Adj $r^2=0.99898429$ FitStdErr=0.03923557 Fstat=2487.5034

a=1.4470162 b=0.033174489 c=-0.18037233 d=0.00080965941

e=-0.0092001993 f=-9.7670671e-06 g=-0.00010045116

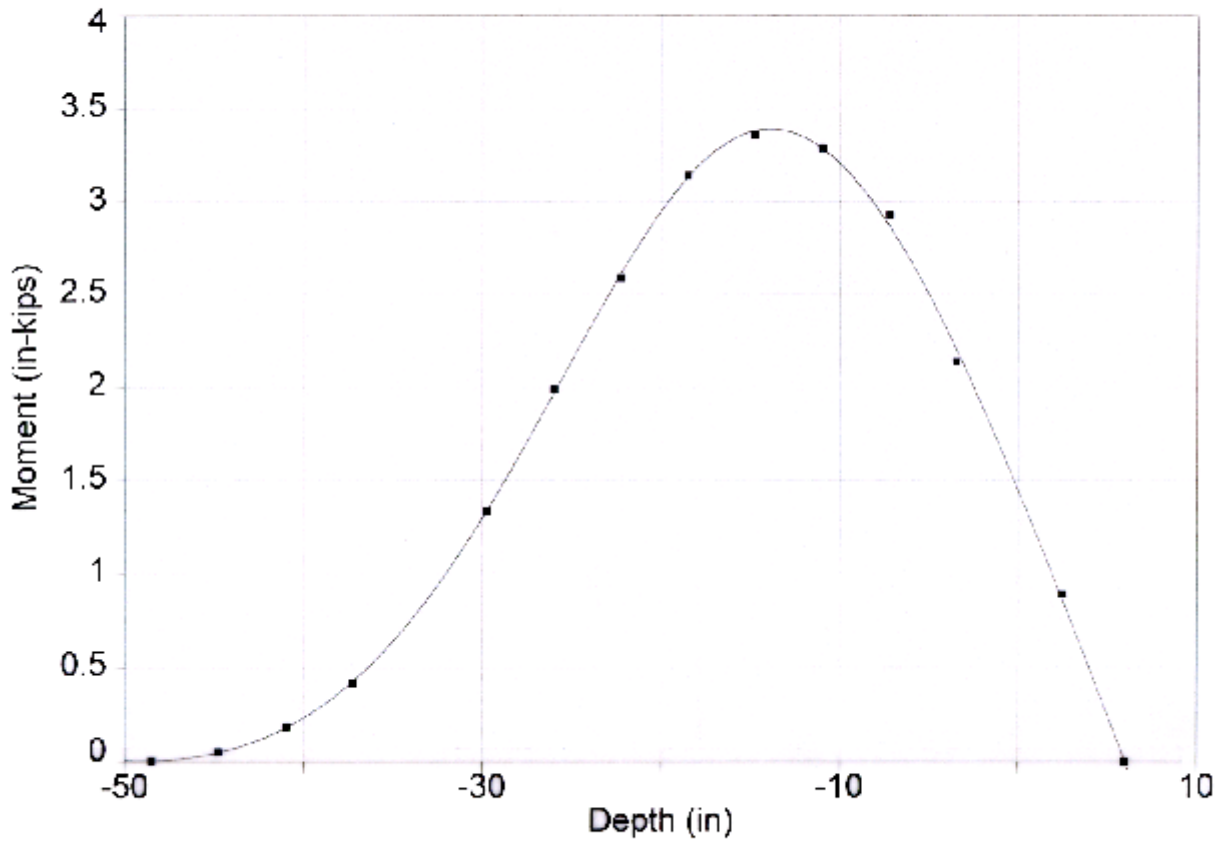


Figure 30. Best Fit Polynomial for Moment Distribution, Lateral Load, 266.7 lbs

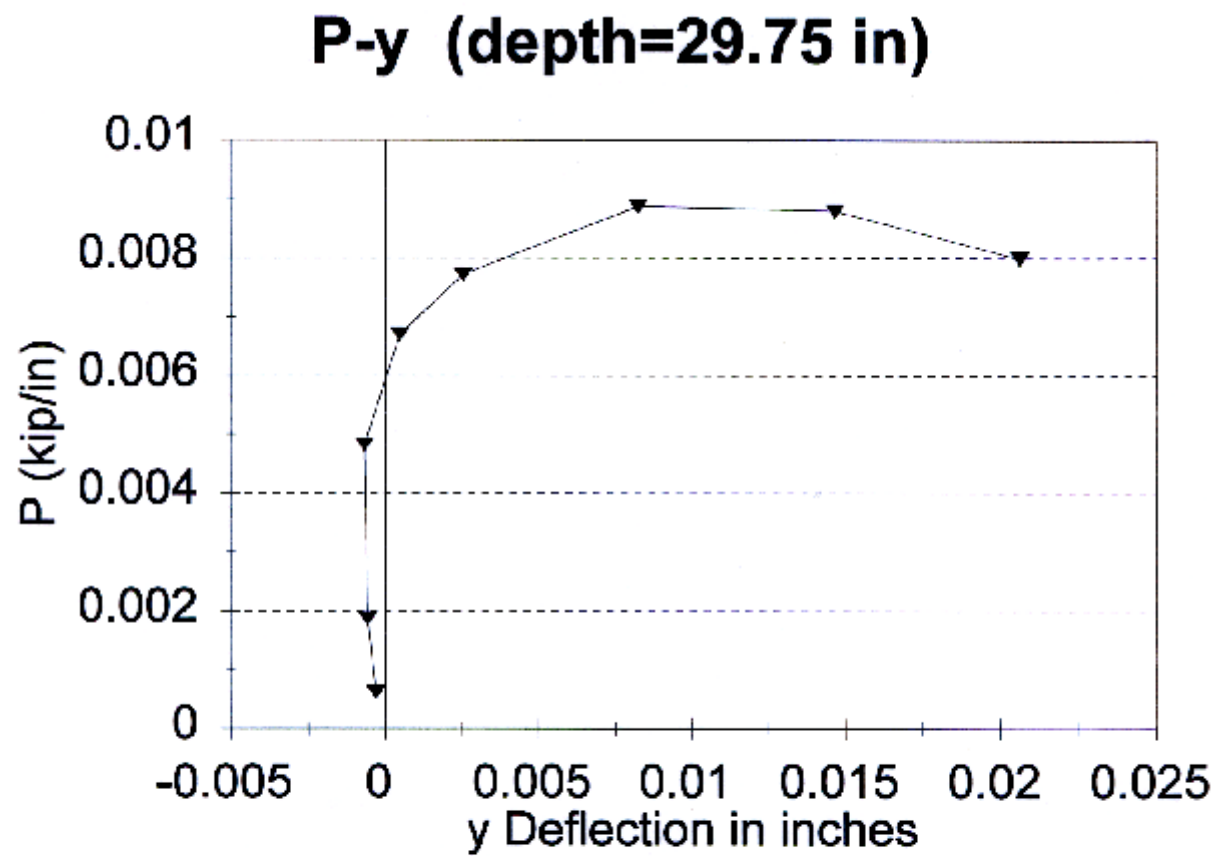


Figure 31. P-y Curve at Depth of 29.75 inches

Shear Strength Profile

Pile Tests #1, 2, & 3

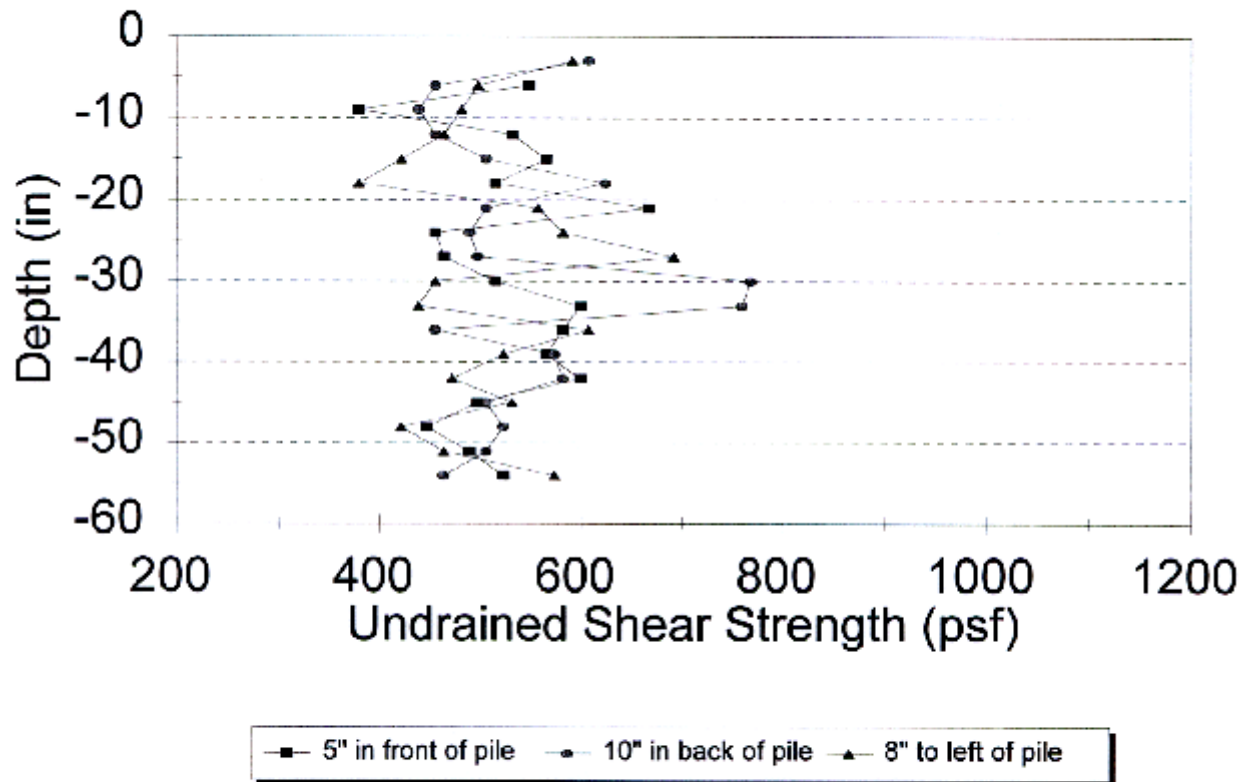


Figure 32. Undrained Shear Strength of Model Clay Soil, Tests 1, 2, & 3

Shear Strength Profile

Pile Tests #4, 5, & 6

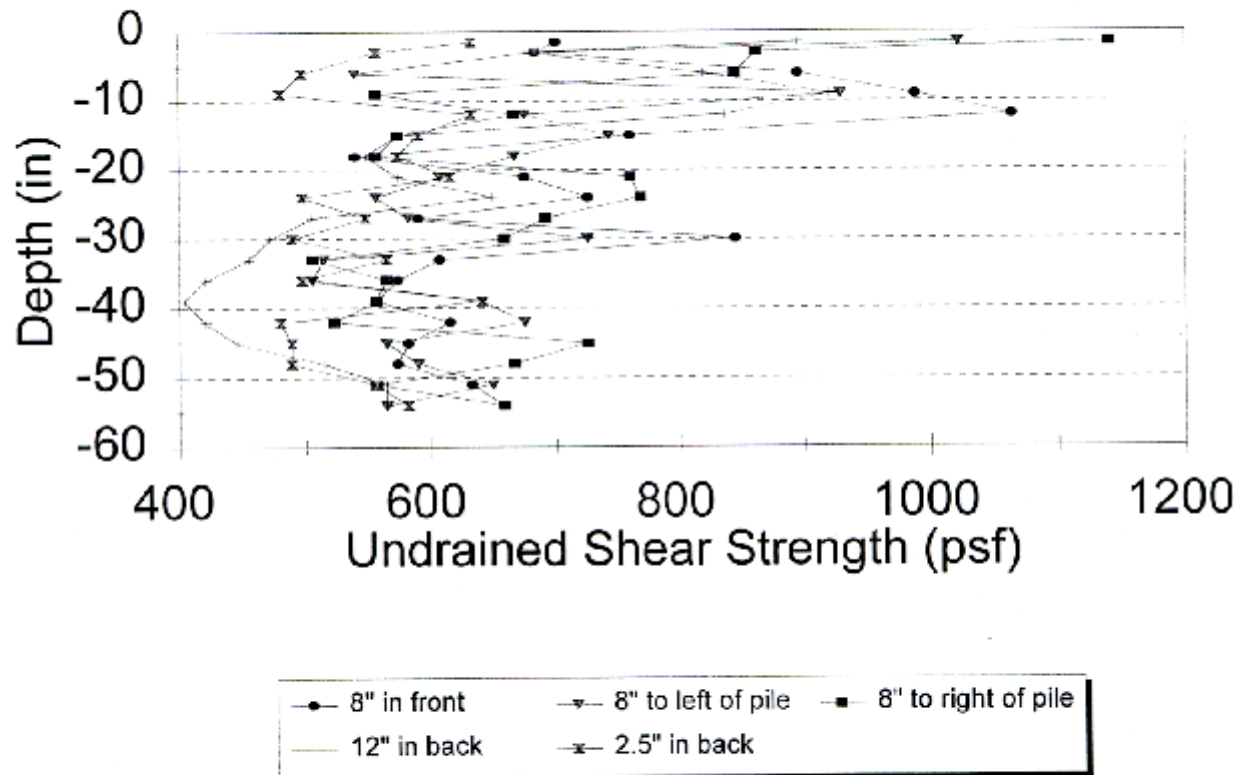


Figure 33. Undrained Shear Strength of Model Clay Soil, Tests 4, 5, & 6

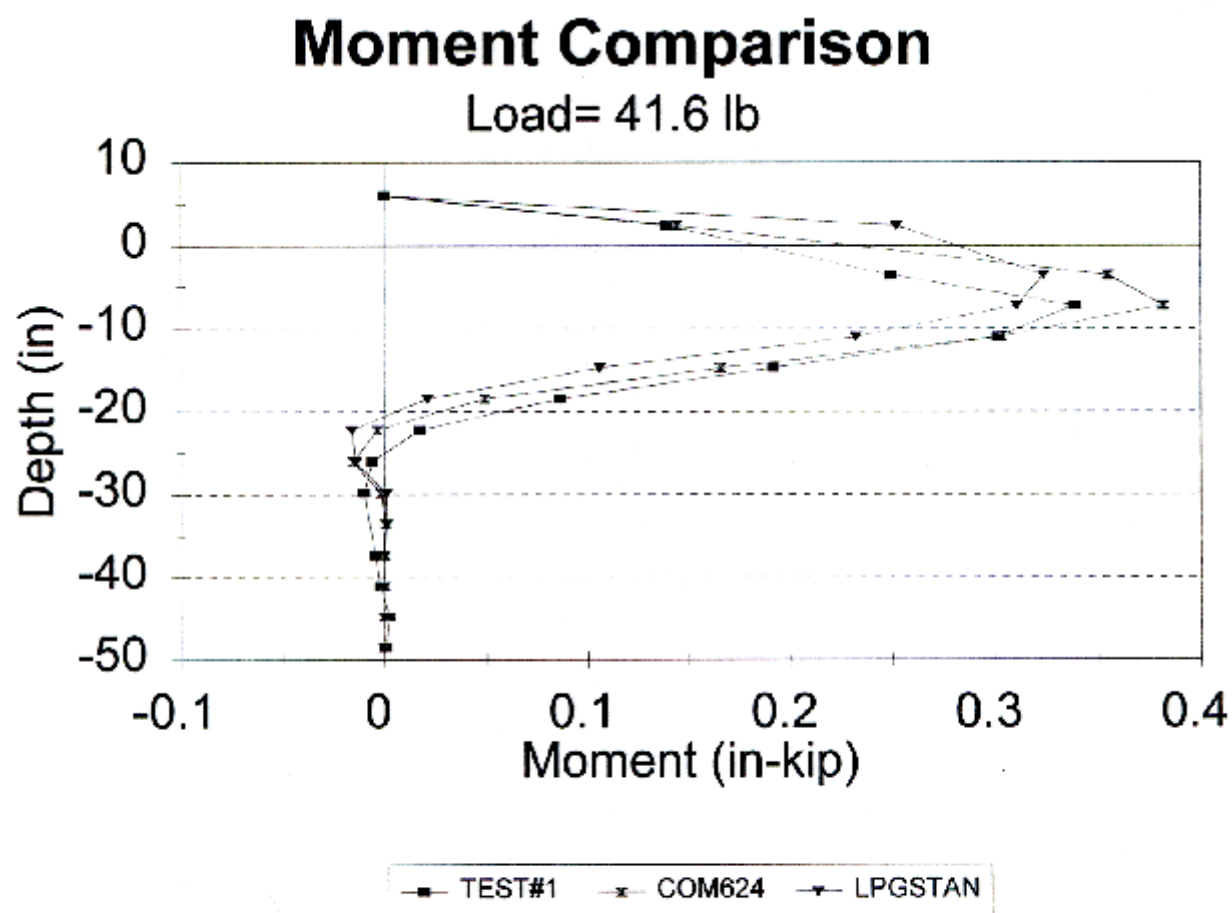


Figure 34. Measured Moments vs. Predicted Moments Lateral Load, 41.6 lbs

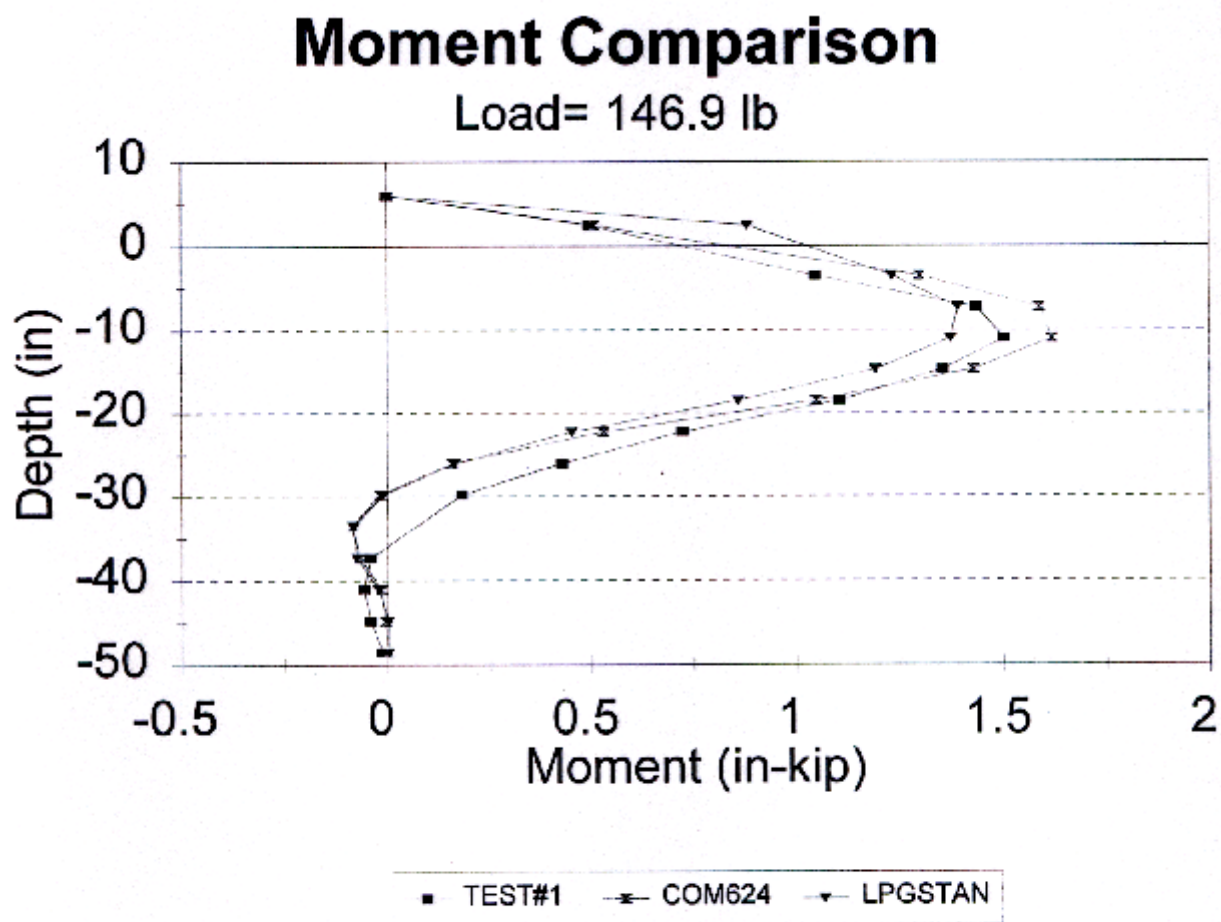


Figure 35. Measured Moments vs. Predicted Moments Lateral Load, 146.9 lbs

Moment Comparison

Load= 179.5 lb

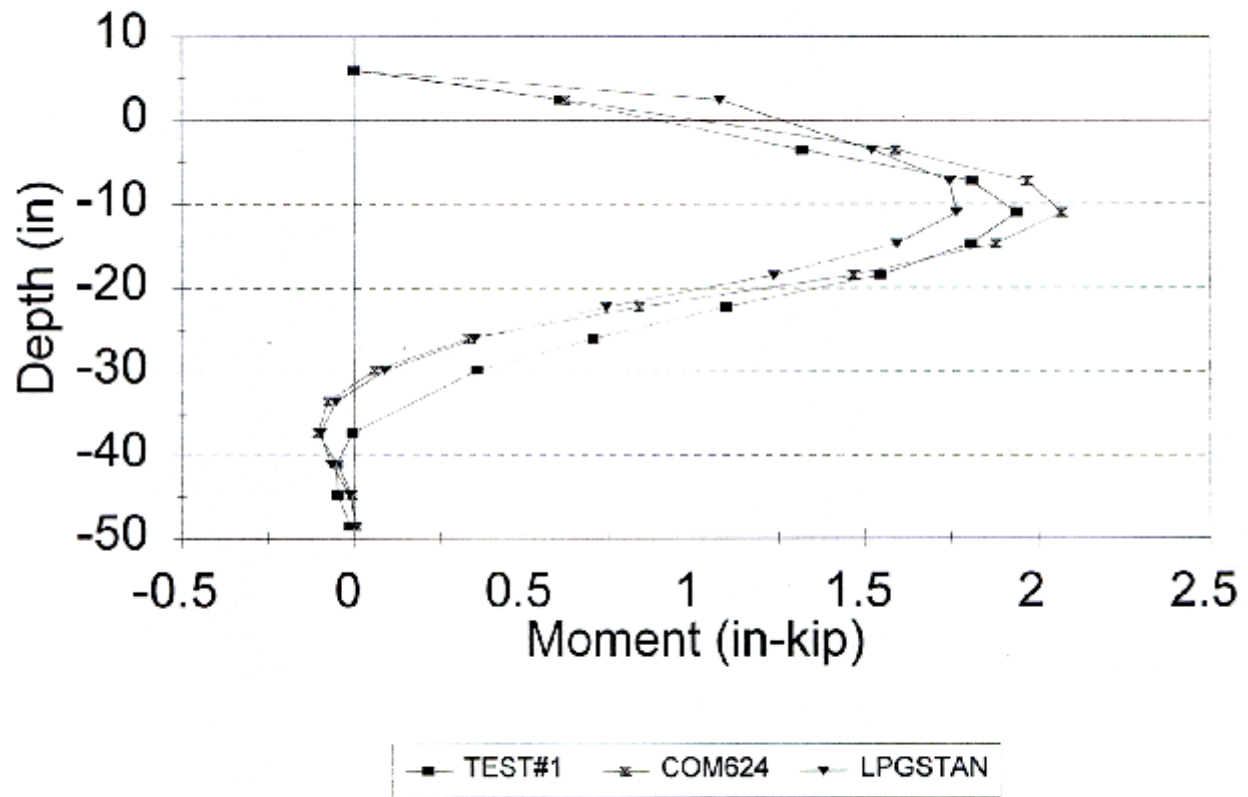


Figure 36. Measured Moments vs. Predicted Moments Lateral Load, 179.5 lbs

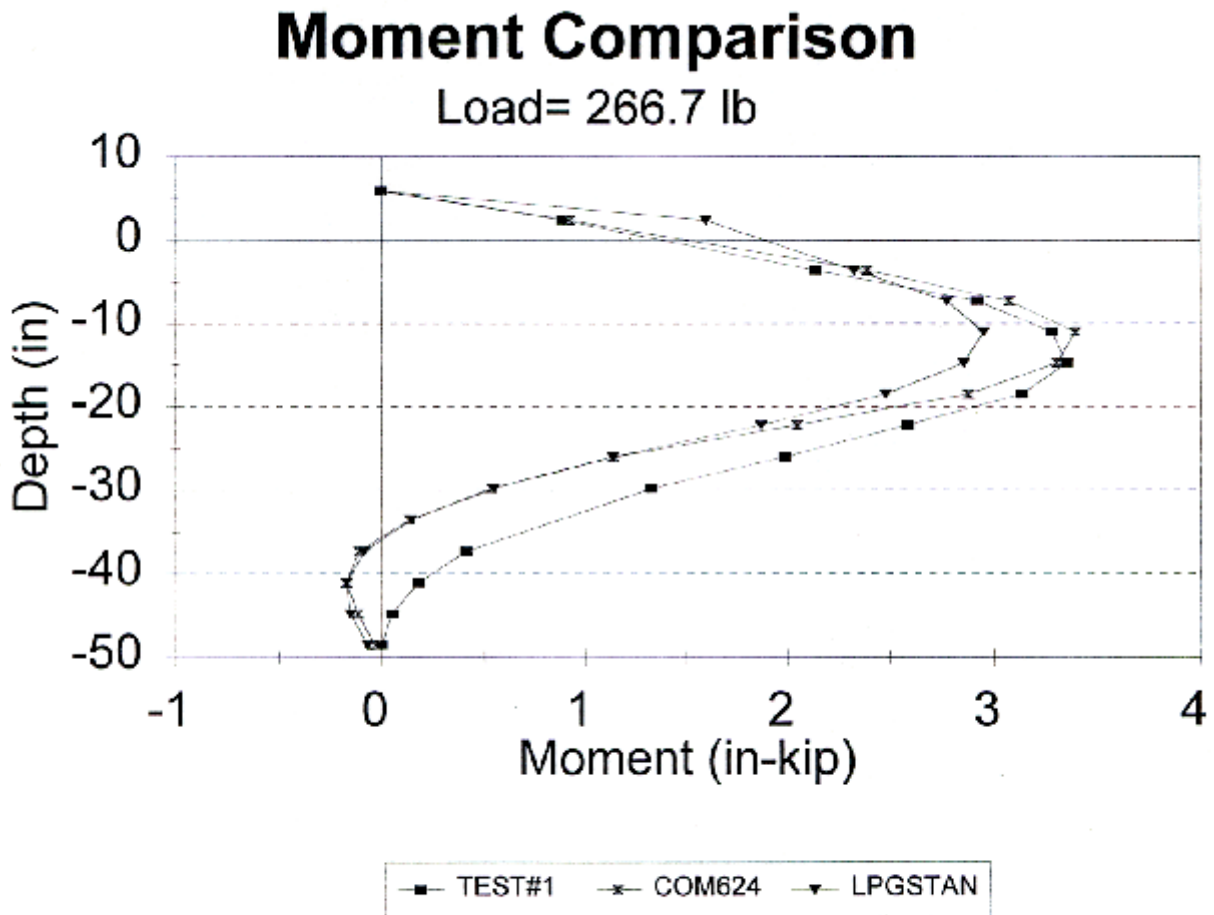


Figure 37. Measured Moments vs. Predicted Moments Lateral Load, 266.7 lbs

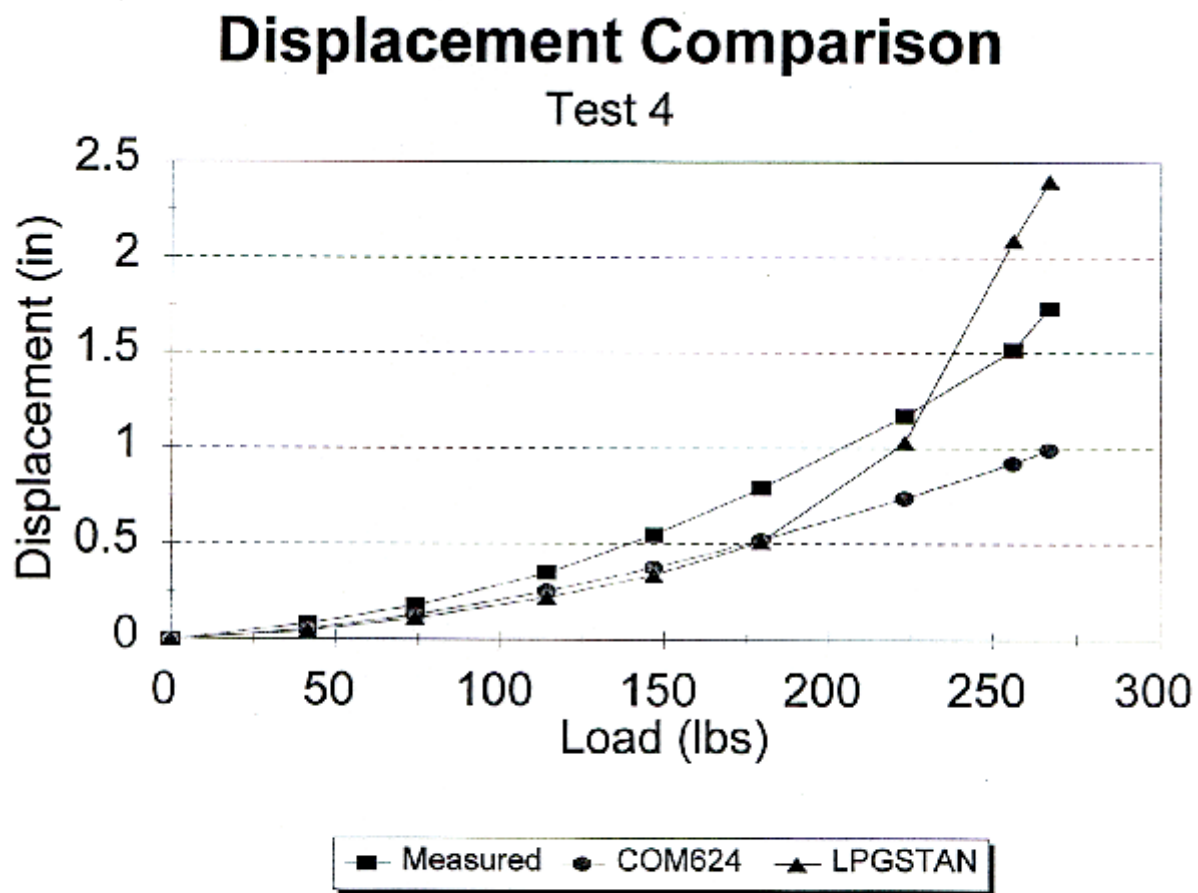


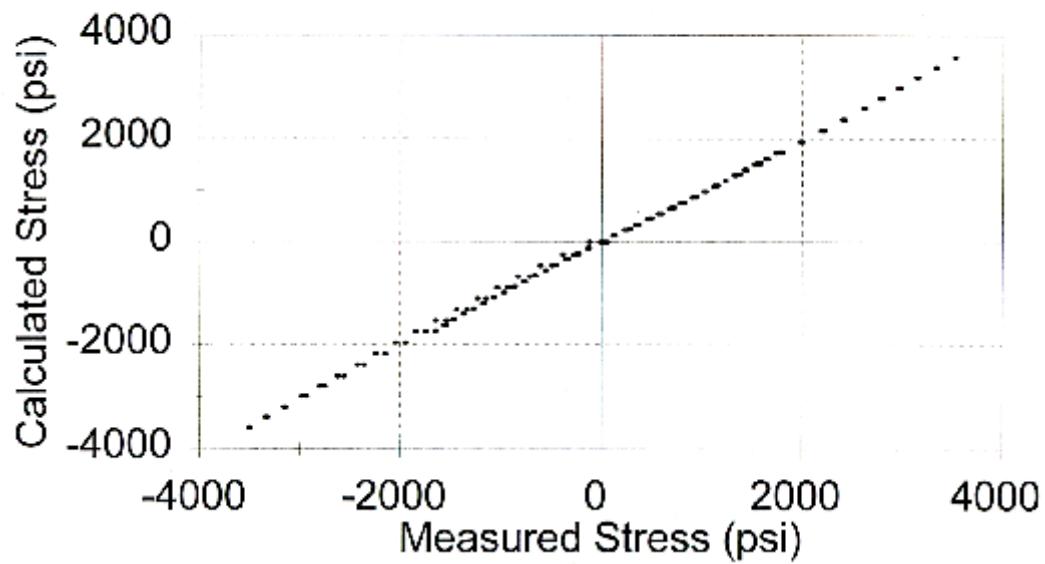
Figure 38. Measured and Predicted Pile Top Displacement vs. Lateral Loads

APPENDIX

Calibration Curves for Each Strain Gage

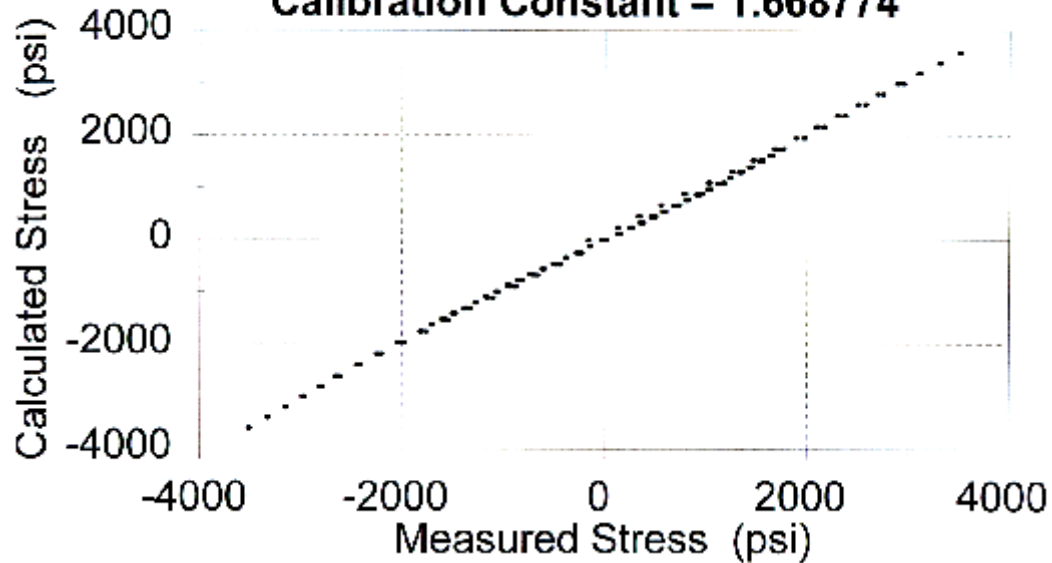
Pile # 2 - Red Gage # 1

Calibration Constant = 1.2377991



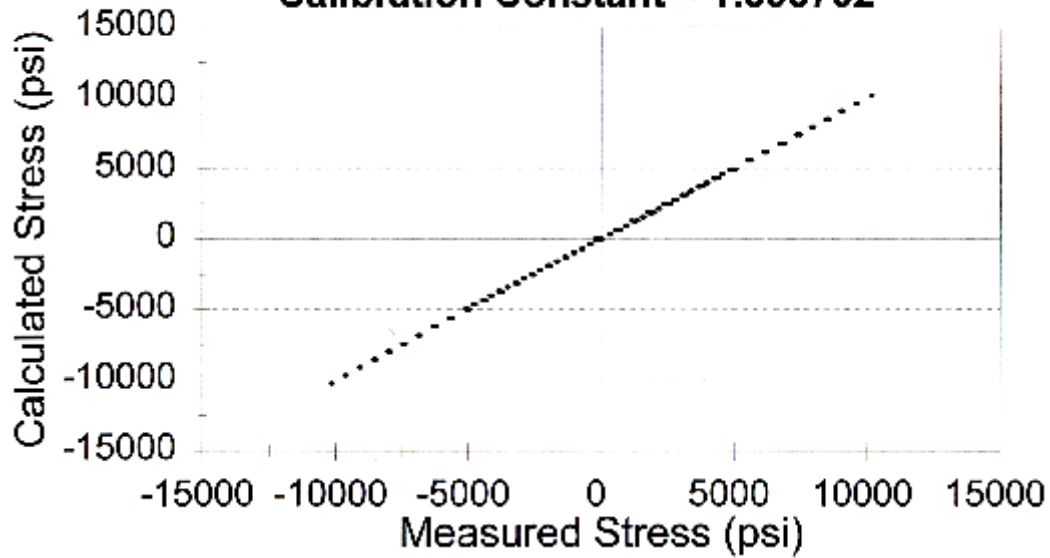
Pile # 2 - Black Gage # 1

Calibration Constant = 1.668774



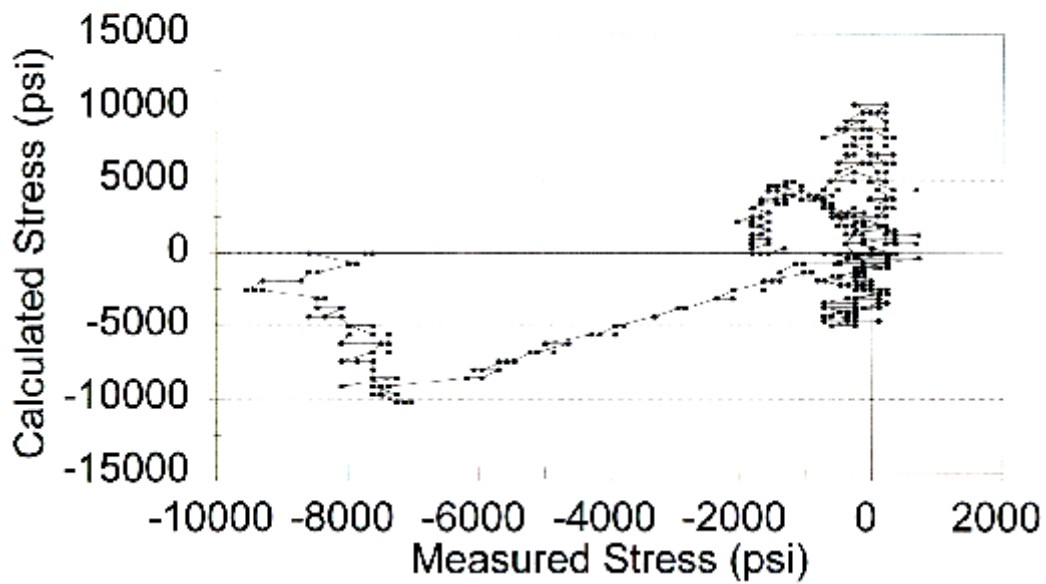
Pile #2 - Red Gage # 2

Calibration Constant = 1.593702

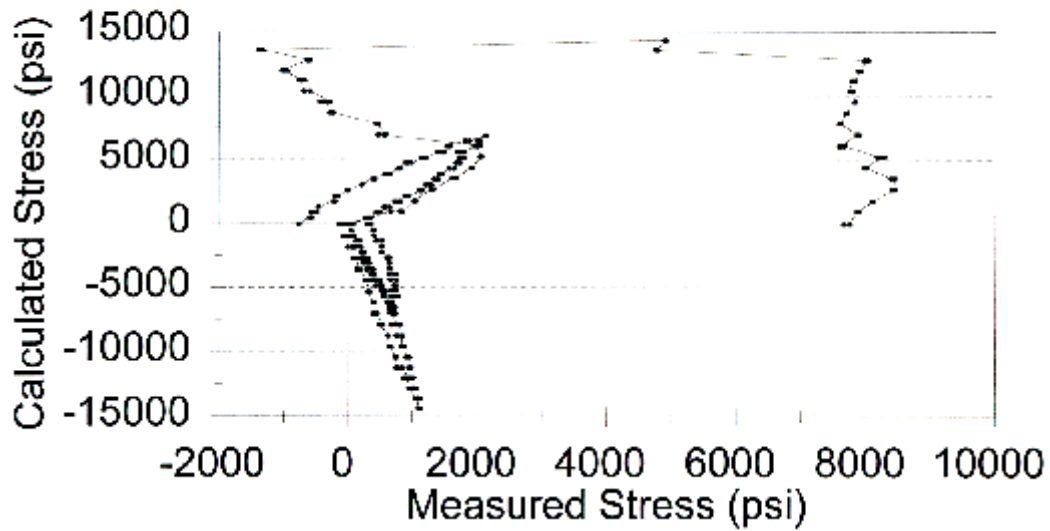


Pile # 2 - Black Gage # 2

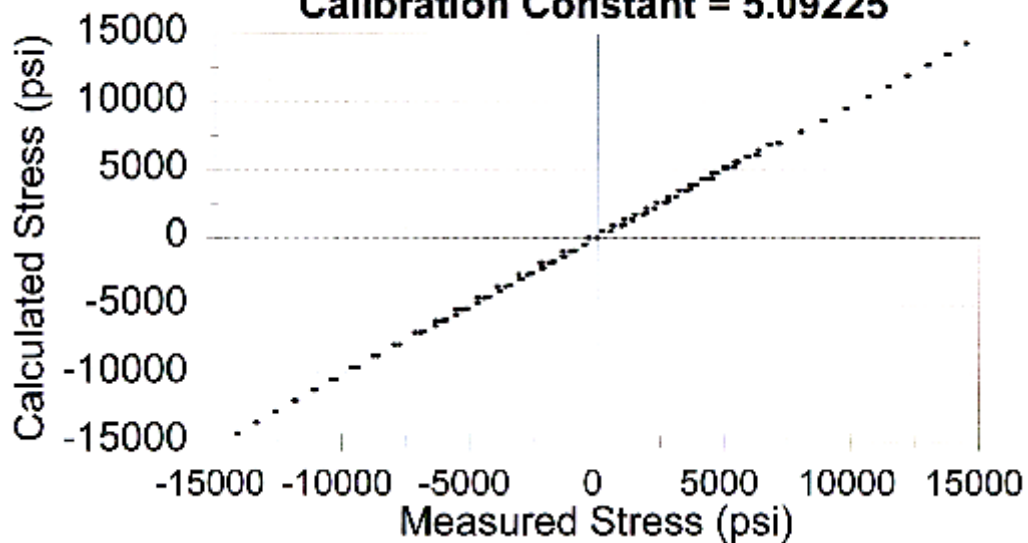
Defective Gage



Pile # 2 - Red Gage # 3 Defective Gage

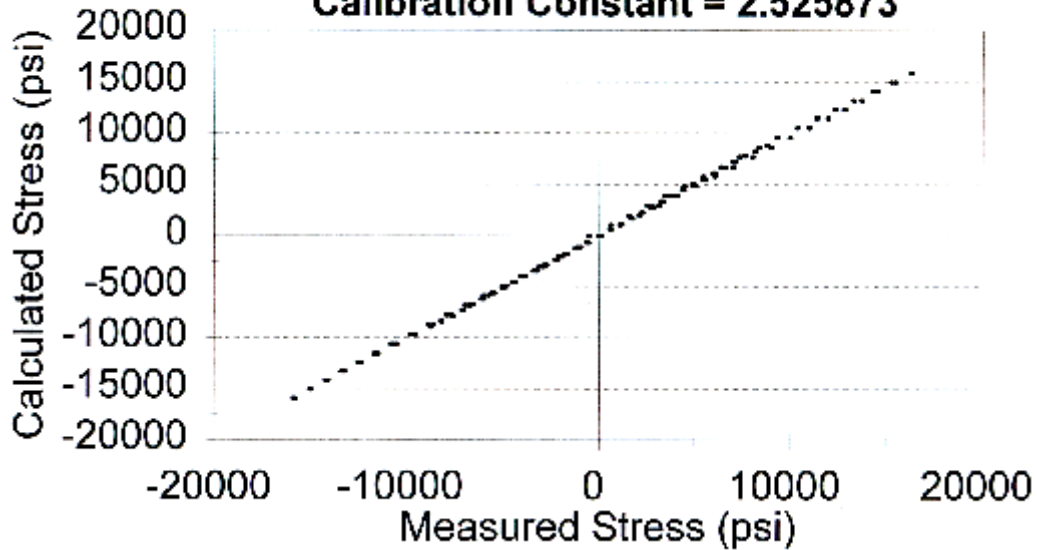


Pile # 2 - Black Gage # 3 Calibration Constant = 5.09225



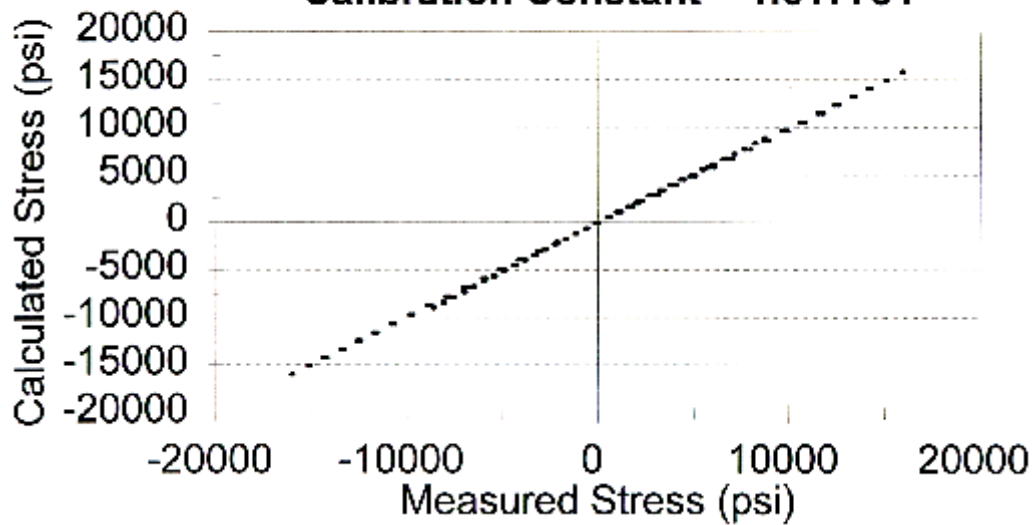
Pile # 2 - Red Gage # 4

Calibration Constant = 2.525873



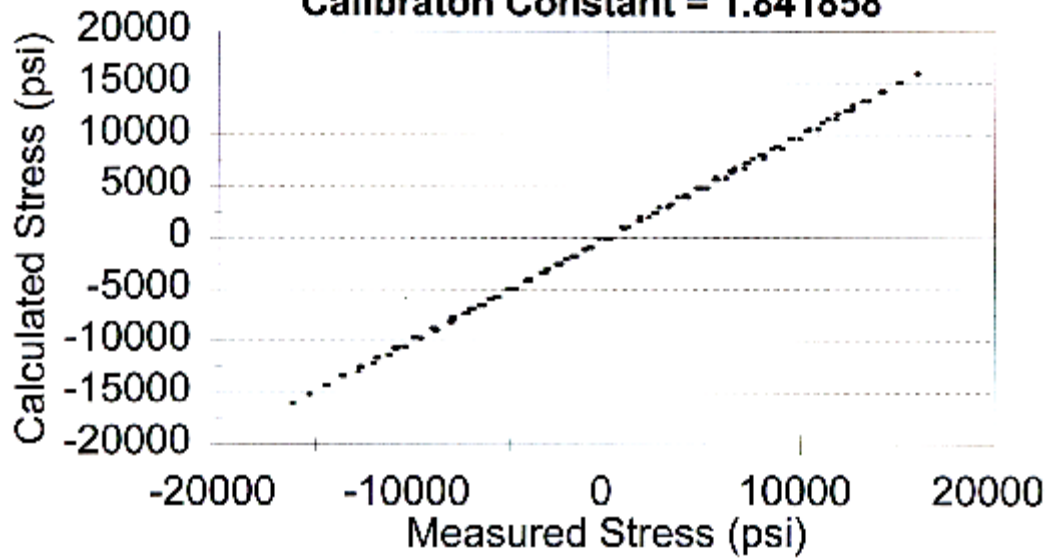
Pile # 2 - Black Gage # 4

Calibration Constant = 1.617731



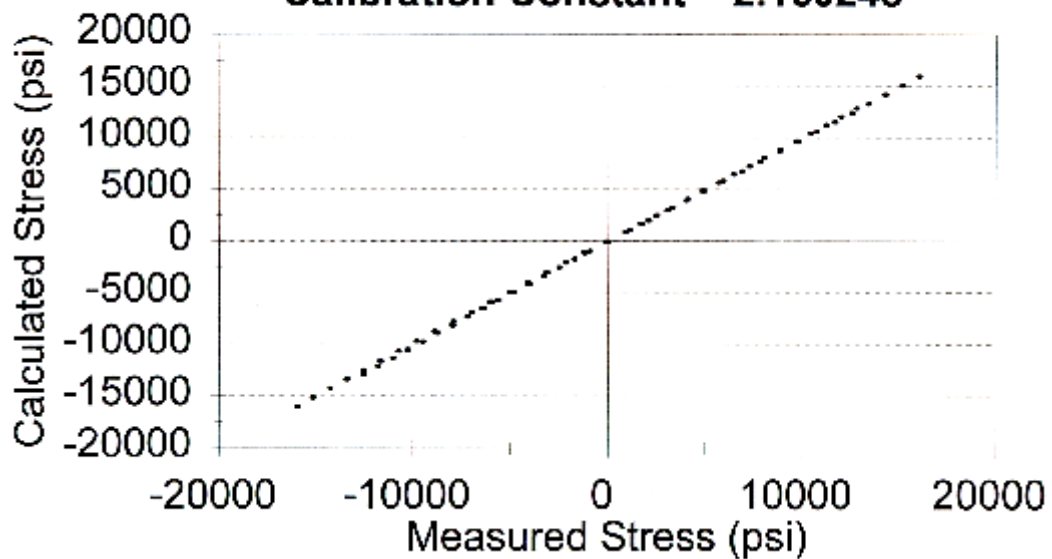
Pile # 2 - Red Gage # 5

Calibration Constant = 1.841858



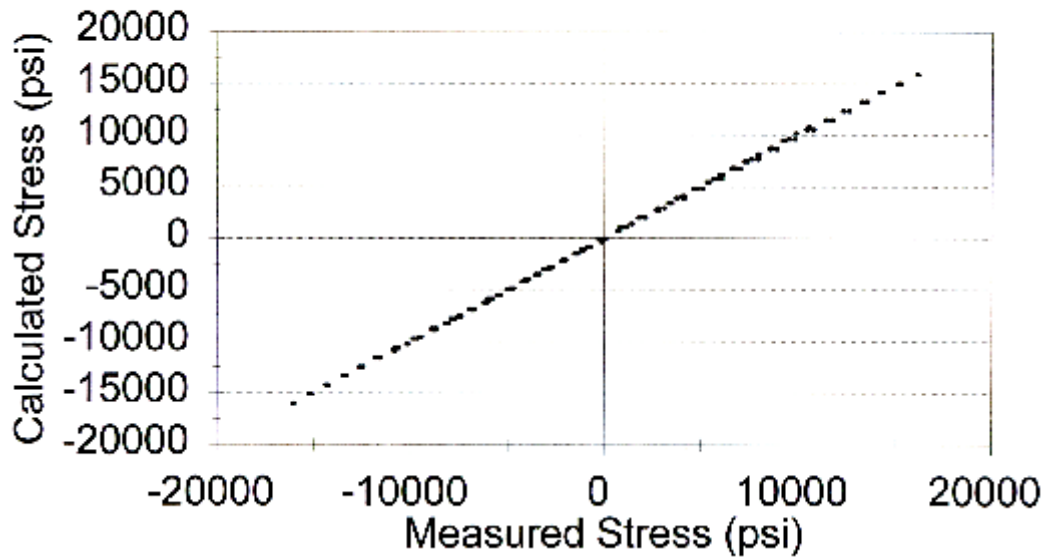
Pile # 2 - Black Gage # 5

Calibration Constant = 2.160248



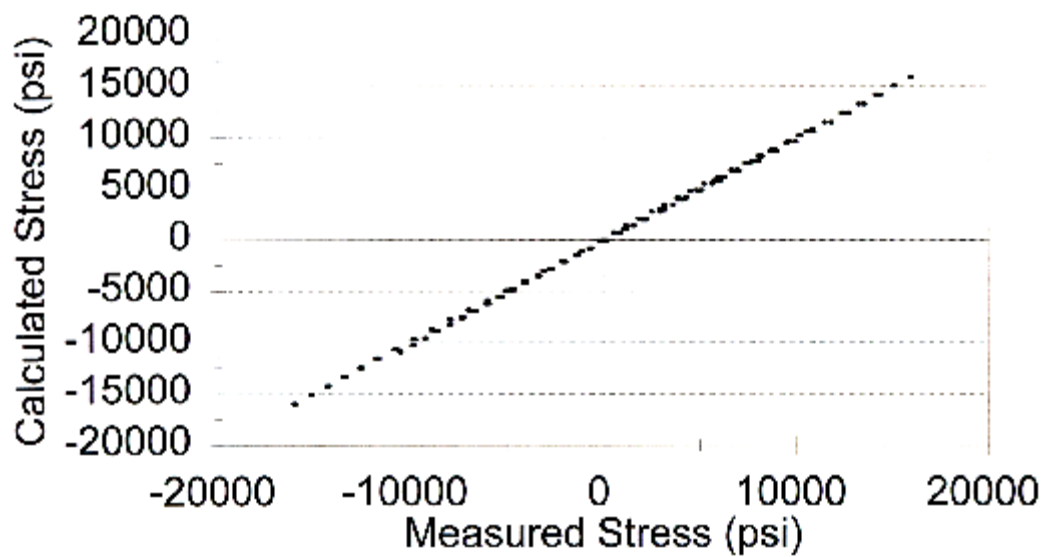
Pile # 2 - Red Gage # 6

Calibration Constant = 1.764209



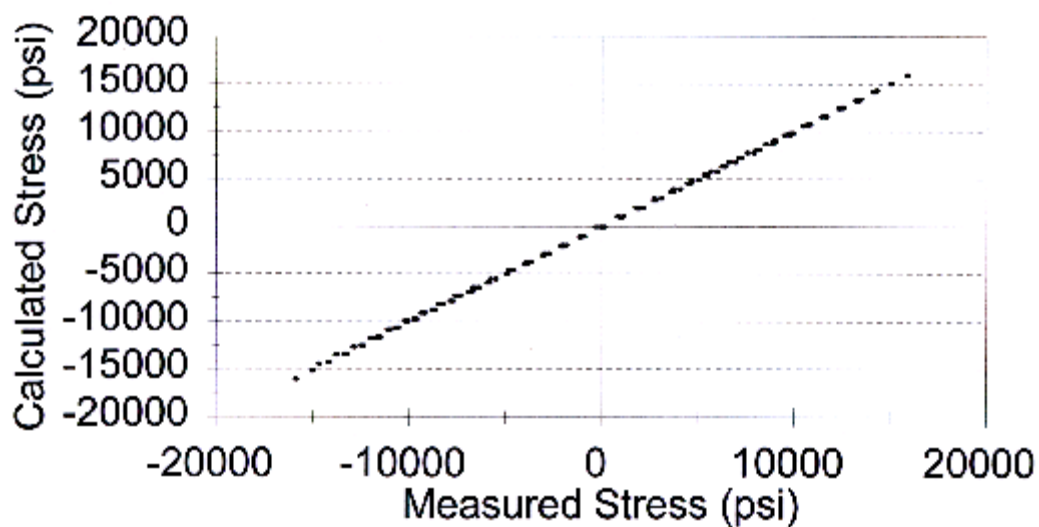
Pile # 2 - Black Gage # 6

Calibration Constant = 1.082606



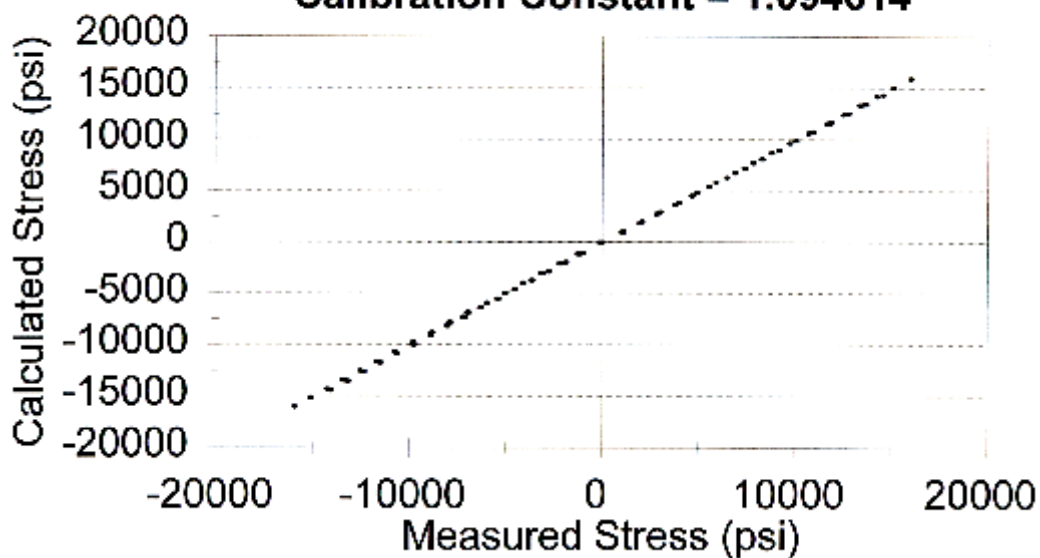
Pile # 2 - Red Gage # 7

Calibration Constant = 1.380346

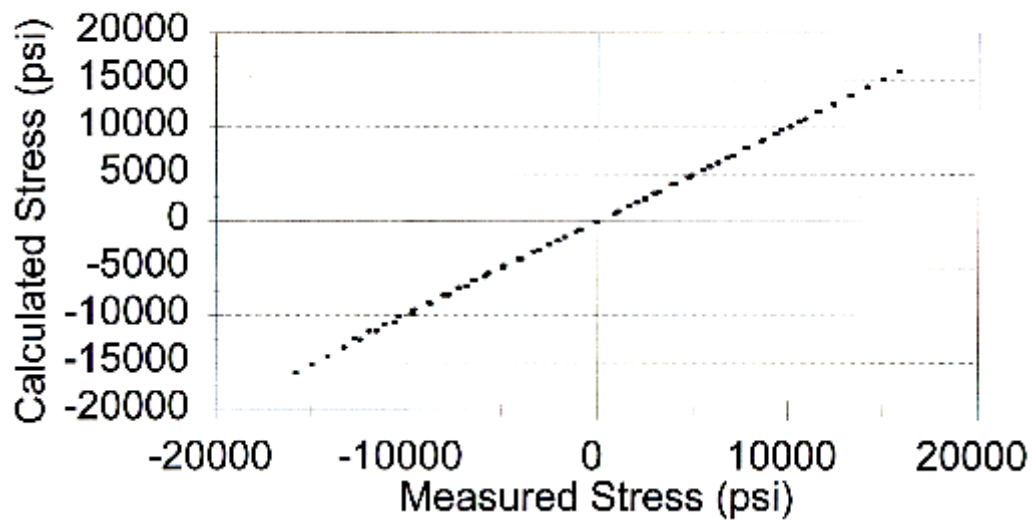


Pile # 2 - Black Gage # 7

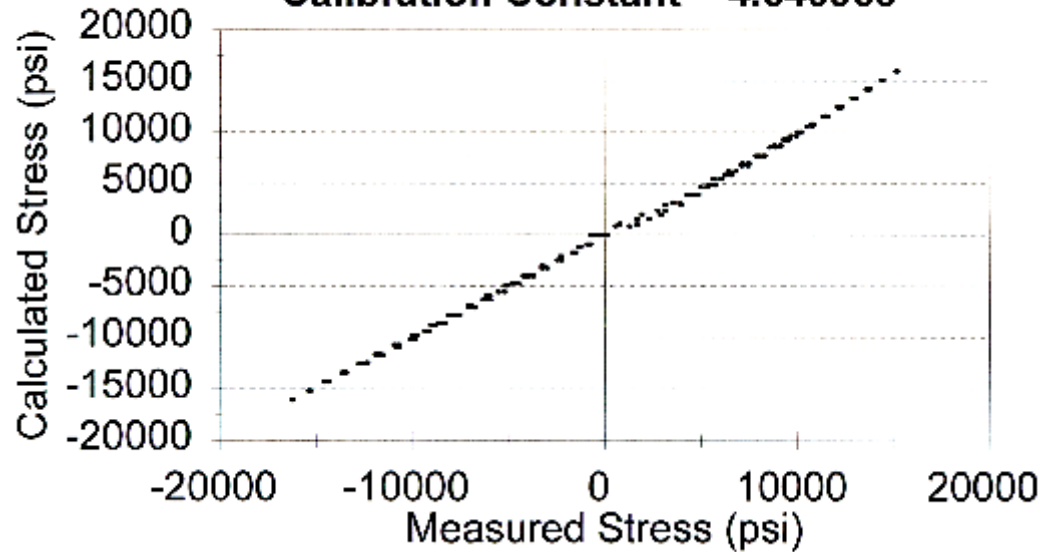
Calibration Constant = 1.094614



Pile # 2 - Red Gage # 8
Calibration Constant = 1.089462

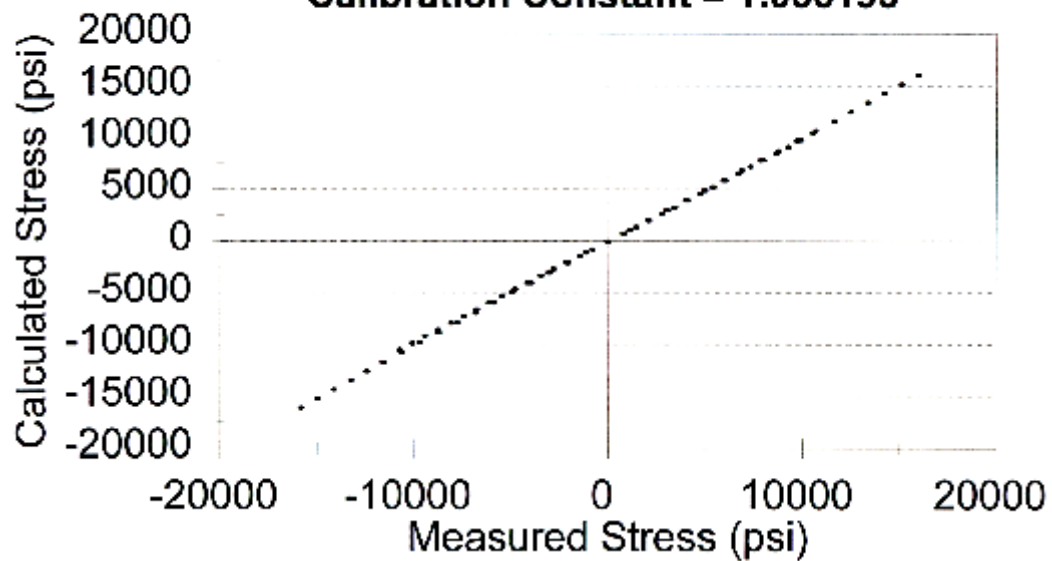


Pile # 2 - Black Gage # 8
Calibration Constant = 4.640968



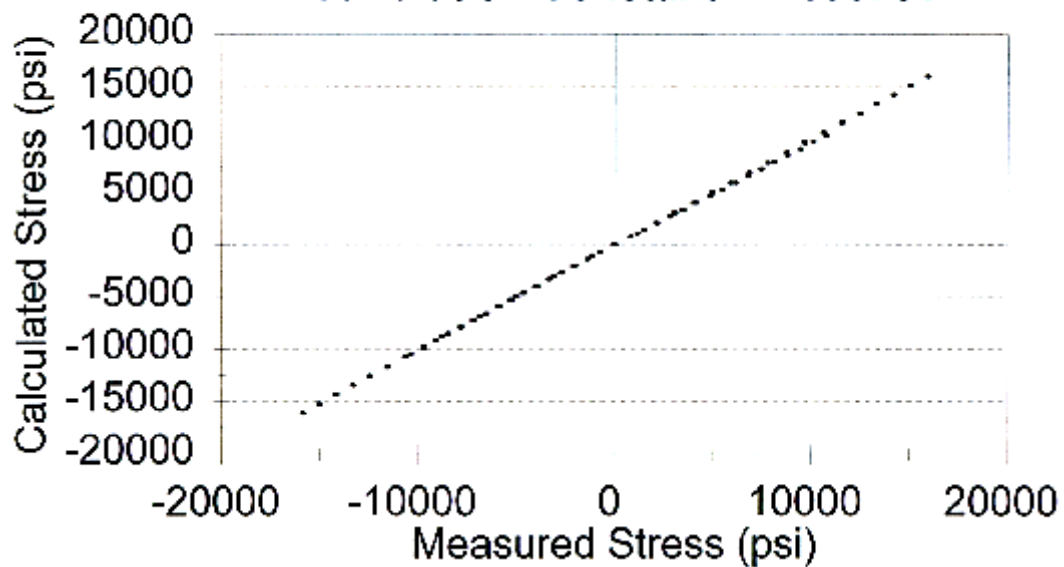
Pile # 2 - Red Gage # 9

Calibration Constant = 1.056193

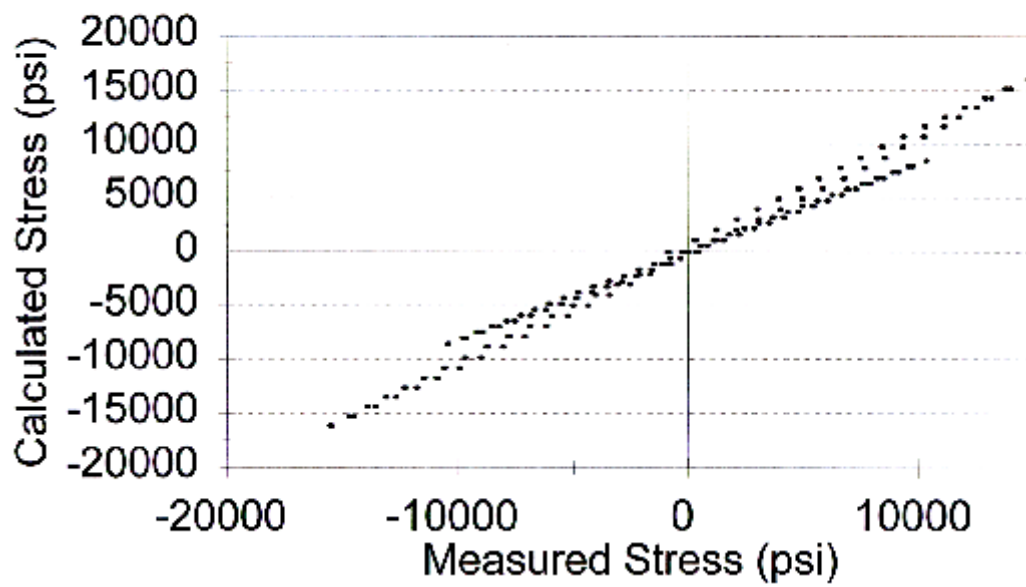


Pile # 2 - Black Gage # 9

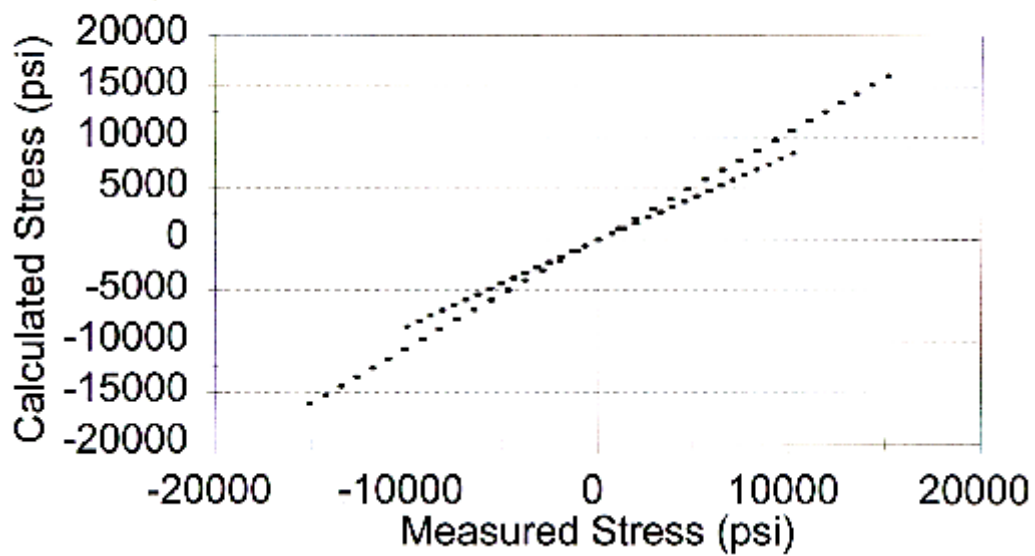
Calibration Constant = 1.098781



Pile # 2 - Red # 10

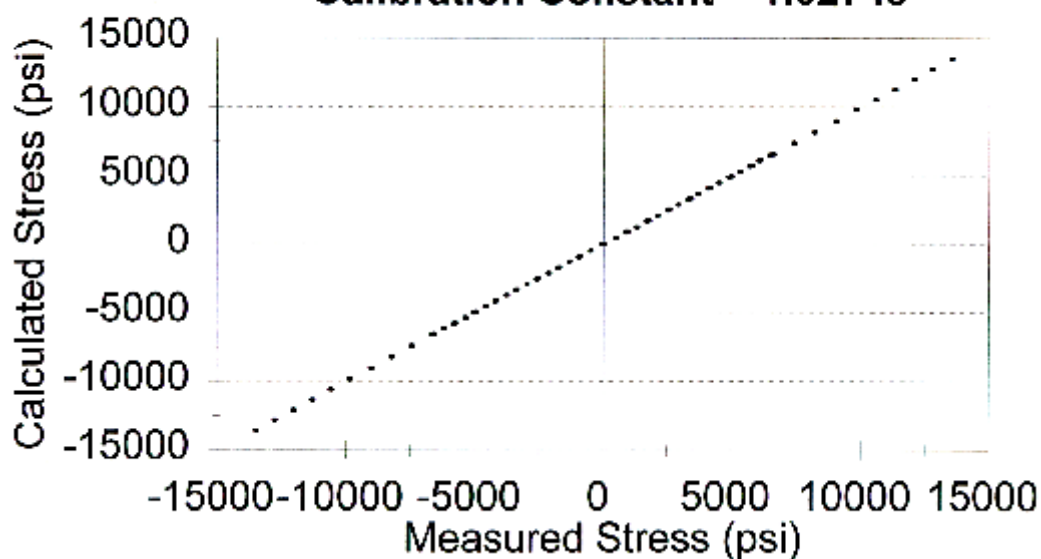


Pile # 2 - Black Gage # 10



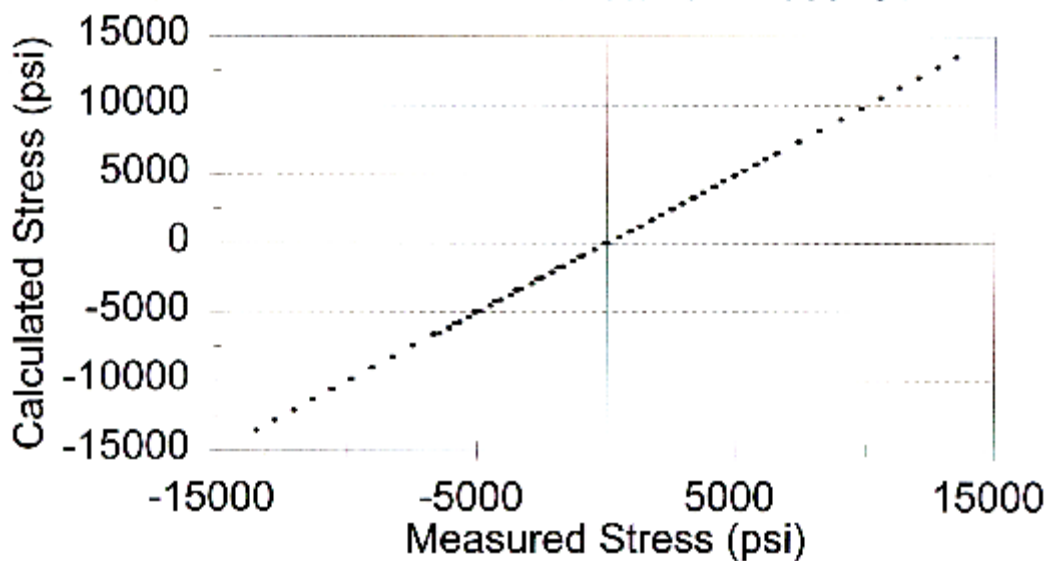
Pile # 2 - Red Gage # 11

Calibration Constant = 1.02748



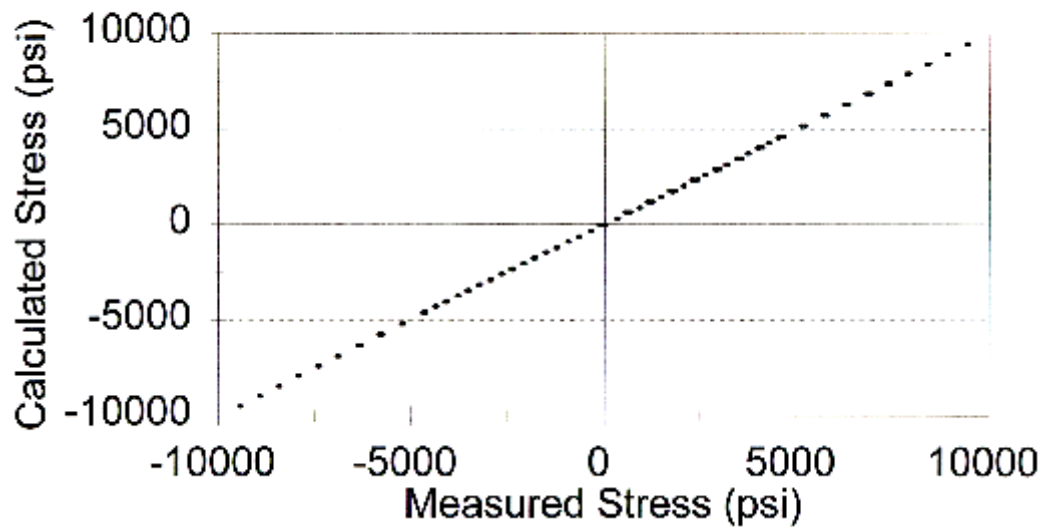
Pile # 2 - Black Gage # 11

Calibration Constant = 1.039251



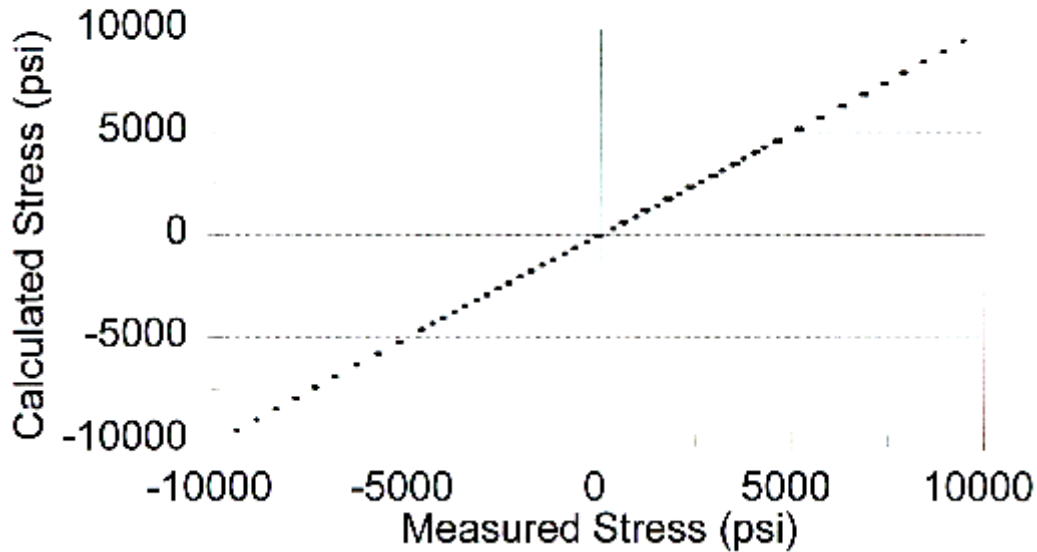
Pile # 2 - Red Gage # 12

Calibration Constant = 1.209876



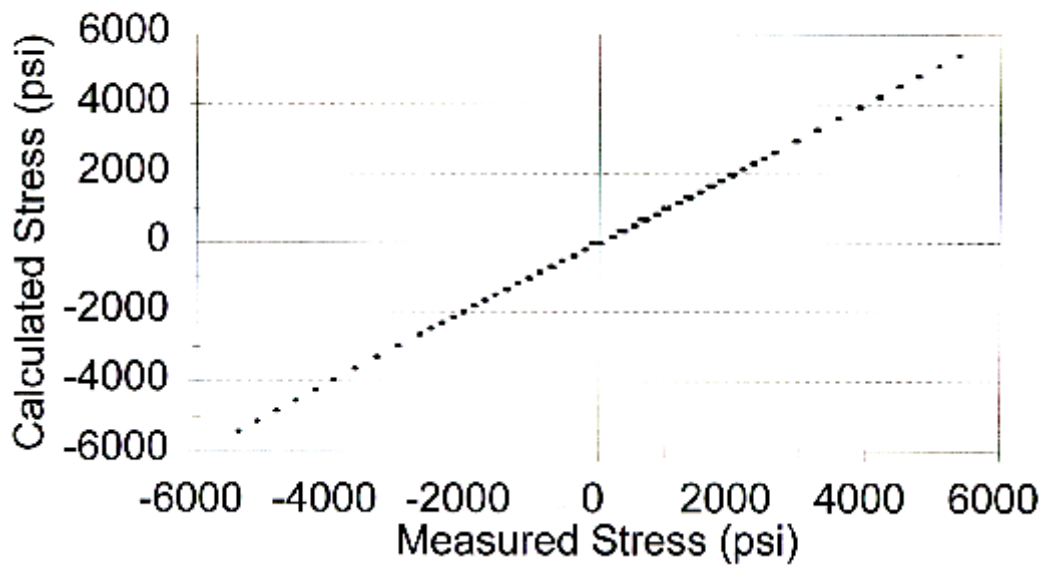
Pile # 2 - Black Gage # 12

Calibration Constant = 1.078021



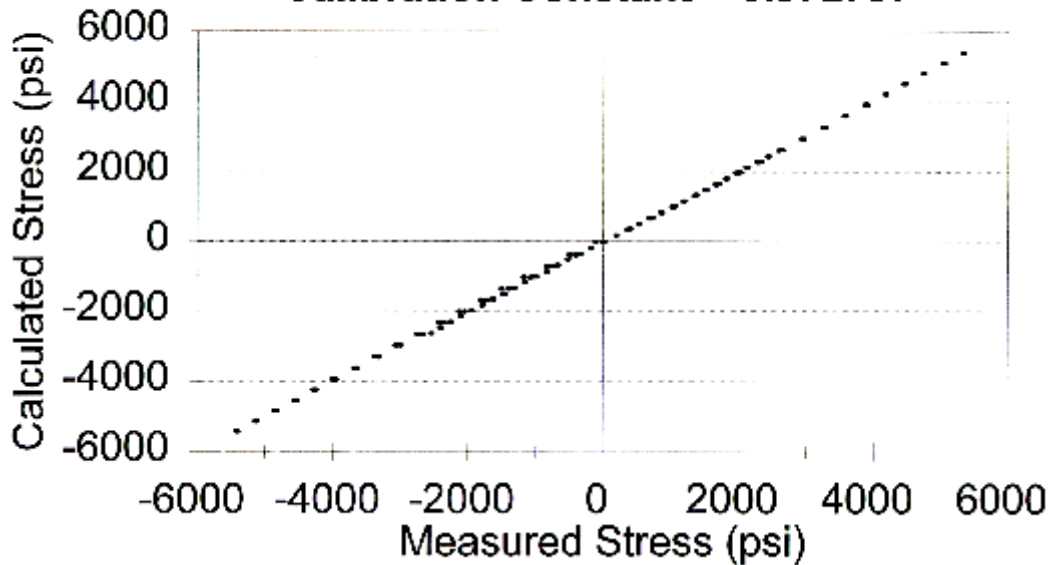
Pile # 2- Red Gage # 13

Calibration Constant = 1.063086



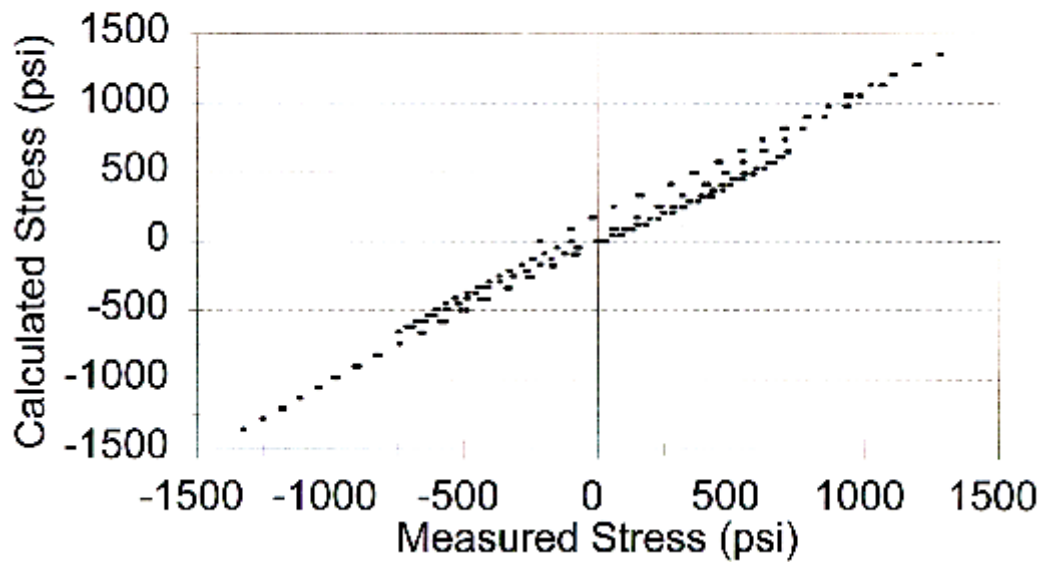
Pile # 2 - Black Gage # 13

Calibration Constant = 0.972797



Pile # 2 - Red Gage # 14

Calibration Constant = 2.496892



Pile # 2 - Black Gage # 14

Calibration Constant = 1.059323

